On the Global Attractor of 2D Incompressible Turbulence with Random Forcing

Pedram Emami, John C. Bowman*

Department of Mathematical and Statistical Sciences, University of Alberta, Edmonton, Alberta T6G 2G1, Canada

Abstract

This study revisits bounds on the projection of the global attractor in the energy–enstrophy plane for 2D incompressible turbulence [Dascaliuc, Foias, and Jolly 2005, 2010]. In addition to providing more elegant proofs of some of the required nonlinear identities, the treatment is extended from the case of constant forcing to the more realistic case of random forcing. Numerical simulations in particular often use a stochastic white-noise forcing to achieve a prescribed mean energy injection rate. The analytical bounds are demonstrated numerically for the case of white-noise forcing.

Keywords: energy, enstrophy, global attractor, two-dimensional turbulence, incompressible turbulence, random forcing

1. Introduction

Turbulence is sometimes characterized as the "last great unsolved problem of classical mechanics." Attempts to understand and predict turbulent flow have been undertaken since the very beginning of the emergence of classical mechanics. While there have been some influential breakthroughs in the last century by great researchers like Taylor, Kolmogorov, Kraichnan, Batchelor, Leith, Ruelle, Takens, Orszag, Frisch and others, the problem of turbulence is complicated enough that there is not even a unified model adopted by all researchers in the field. The nature of turbulence is still controversial. Is it a deterministic or stochastic phenomenon? Even with the emergence

*Corresponding author

URL: `http://www.math.ualberta.ca/$\sim $bowman` (John C. Bowman)

of chaos theory in the 1980s and the understanding of nonlinear dynamical systems using the concepts of attractors, basins, intermittency, and coherent structures, the problem of turbulence has not been precisely described. The complex nature and essence of turbulence deserves much further study. In this work we apply tools from functional analysis to study turbulence as a deterministic phenomenon governed by the Navier–Stokes equations, but driven by a stochastic forcing.

2. Definitions and preliminaries

One of the simplest contexts in which to pose the turbulence problem is 2D incompressible homogeneous isotropic turbulent flow in a bounded domain with periodic boundary conditions and no mean velocity and forcing. One close realization of this ideal form of turbulence in laboratories is a very thin layer of turbulent fluid far downstream from a flow passing over a net of wires.

Looking at this ideal form of turbulence deterministically involves using the incompressible Navier–Stokes and continuity equations expressed as a set of integro-differential equations, with zero mean flow and forcing, along with constant density $\rho = 1$:

$$\frac{\partial \boldsymbol{u}}{\partial t} - \nu \nabla^2 \boldsymbol{u} + \boldsymbol{u} \cdot \boldsymbol{\nabla} \boldsymbol{u} + \boldsymbol{\nabla} p = \boldsymbol{F}, \tag{1}$$

$$\boldsymbol{\nabla} \cdot \boldsymbol{u} = 0, \tag{2}$$

$$\int_\Omega \boldsymbol{u} \, d\boldsymbol{x} = \boldsymbol{0}, \qquad \int_\Omega \boldsymbol{F} \, d\boldsymbol{x} = \boldsymbol{0}, \tag{3}$$

$$\boldsymbol{u}(\boldsymbol{x}, 0) = \boldsymbol{u}_0(\boldsymbol{x}), \tag{4}$$

with $\Omega = [0, L] \times [0, L]$ and periodic boundary conditions on $\partial\Omega$. This problem can be considered in a specific Hilbert space (H) with the standard L^2 inner product

$$(\boldsymbol{u}, \boldsymbol{v}) = \int_\Omega \boldsymbol{u}(\boldsymbol{x}) \cdot \boldsymbol{v}(\boldsymbol{x}) \, d\boldsymbol{x}, \quad \text{where} \quad \boldsymbol{a} \cdot \boldsymbol{b} = \sum_i a_i b_i.$$

The Hilbert space is defined as

$$H(\Omega) \doteq \mathrm{cl} \left\{ \boldsymbol{u} \in (C^2(\Omega) \cap L^2(\Omega))^2 \mid \boldsymbol{\nabla} \cdot \boldsymbol{u} = 0, \ \int_\Omega \boldsymbol{u} \, d\boldsymbol{x} = \boldsymbol{0} \right\}, \tag{5}$$

with L^2 norm

$$|\boldsymbol{u}| = (\boldsymbol{u}, \boldsymbol{u})^{1/2} = \left(\int_\Omega \boldsymbol{u}(\boldsymbol{x}, t) \boldsymbol{\cdot} \boldsymbol{u}(\boldsymbol{x}, t) \, d\boldsymbol{x} \right)^{1/2}$$

(here $\doteq$ is used to emphasize a definition and cl denotes the closure with respect to the L^2 norm). The above problem can then be expressed as

$$\frac{d\boldsymbol{u}}{dt} - \nu \nabla^2 \boldsymbol{u} + \boldsymbol{u} \boldsymbol{\cdot} \boldsymbol{\nabla} \boldsymbol{u} + \boldsymbol{\nabla} p = \boldsymbol{F}, \qquad \boldsymbol{u}(t) \in H(\Omega). \tag{6}$$

Let $A \doteq -\mathcal{P}(\nabla^2)$, $\boldsymbol{f} \doteq \mathcal{P}(\boldsymbol{F})$, and define the bilinear map

$$\mathcal{B}(\boldsymbol{u}, \boldsymbol{u}) \doteq \mathcal{P} \left(\boldsymbol{u} \boldsymbol{\cdot} \boldsymbol{\nabla} \boldsymbol{u} + \boldsymbol{\nabla} p \right),$$

where $\mathcal{P}$ is the Helmholtz–Leray projection operator on $H(\Omega)$:

$$\mathcal{P}(\boldsymbol{v}) \doteq \boldsymbol{v} - \boldsymbol{\nabla} \nabla^{-2} \boldsymbol{\nabla} \boldsymbol{\cdot} \boldsymbol{v}, \qquad \forall \boldsymbol{v} \in H(\Omega).$$

In terms of these definitions, (6) can be written more compactly as

$$\frac{d\boldsymbol{u}}{dt} + \nu A \boldsymbol{u} + \mathcal{B}(\boldsymbol{u}, \boldsymbol{u}) = \boldsymbol{f}. \tag{7}$$

3. Stokes operator $\boldsymbol{A}$

The operator $A = \mathcal{P}(-\nabla^2)$ is positive-semidefinite and self-adjoint in $H(\Omega)$, with a compact inverse whose eigenvalues are

$$\lambda = k_0^2 \boldsymbol{k} \boldsymbol{\cdot} \boldsymbol{k}, \qquad \boldsymbol{k} \in \mathbb{Z} \times \mathbb{Z} \backslash \{\boldsymbol{0}\},$$

where $k_0 = 2\pi/L$. The eigenvalues of a positive-definite infinite-dimensional linear operator can be arranged as

$$0 < \lambda_0 < \lambda_1 < \lambda_2 < \cdots, \qquad \lambda_0 = k_0^2$$

and their eigenvectors, $\boldsymbol{w}_i$, $i \in \mathbb{N}_0$, form an orthonormal basis for the Hilbert space H, upon which we can define any power of A:

$$A^\alpha \boldsymbol{w}_j = \lambda_j^\alpha \boldsymbol{w}_j, \qquad \alpha \in \mathbb{R}, \quad j \in \mathbb{N}_0.$$

Having the above orthonormal basis, it is possible to define a new space $V^{2\alpha} \subset H$ as [19]

$$V^{2\alpha} = D(A^{\alpha}) \doteq \left\{ \boldsymbol{u} \in H \mid \sum_{j=0}^{\infty} \lambda_j^{2\alpha} (\boldsymbol{u}, \boldsymbol{w}_j)^2 < \infty \right\}.$$

We are especially interested in the subspace $V = V^{2(1/2)}$ consisting of solutions in H having finite enstrophy:

$$V = D(A^{1/2}) \doteq \left\{ \boldsymbol{u} \in H \mid \sum_{j=0}^{\infty} \lambda_j (\boldsymbol{u}, \boldsymbol{w}_j)^2 < \infty \right\}.$$

A suitable norm for the elements of V is

$$||\boldsymbol{u}|| = \left| A^{1/2} u \right| = \left(\int_{\Omega} \sum_{i=1}^{2} \frac{\partial \boldsymbol{u}}{\partial x_i} \cdot \frac{\partial \boldsymbol{u}}{\partial x_i} \right)^{1/2} = \left(\sum_{j=0}^{\infty} \lambda_j (\boldsymbol{u}, \boldsymbol{w}_j)^2 \right)^{1/2}.$$

It is essential to exploit properties of the bilinear map $\mathcal{B}$ together with incompressibility and periodicity, along with specific properties of the Stokes operator A. Here we only list the most important properties of the bilinear map and the reader who is interested in their proofs is referred to Appendix A for further details. Specifically, we will need the antisymmetry

$$(\mathcal{B}(\boldsymbol{u}, \boldsymbol{v}), \boldsymbol{w}) = -(\mathcal{B}(\boldsymbol{u}, \boldsymbol{w}), \boldsymbol{v}),$$

orthogonality in 2D,

$$(\mathcal{B}(\boldsymbol{u}, \boldsymbol{u}), A\boldsymbol{u}) = 0, \tag{8}$$

the strong form of enstrophy invariance in a 2D periodic domain,

$$(\mathcal{B}(A\boldsymbol{v}, \boldsymbol{v}), \boldsymbol{u}) = (\mathcal{B}(\boldsymbol{u}, \boldsymbol{v}), A\boldsymbol{v}),$$

and the 2D general identity in a periodic domain,

$$(\mathcal{B}(A\boldsymbol{u}, \boldsymbol{u}), \boldsymbol{u}) + (\mathcal{B}(\boldsymbol{v}, A\boldsymbol{v}), \boldsymbol{u}) + (\mathcal{B}(\boldsymbol{v}, \boldsymbol{v}), A\boldsymbol{v}) = 0.$$

Finally, we state an important Sobolev inequality, the 2D Ladyzhenskaya inequality:

$$|\boldsymbol{u}|_{L^4(\Omega)} \leq C_L |\boldsymbol{u}|^{1/2} ||\boldsymbol{u}||^{1/2}, \tag{9}$$

where the constant C_L depends only on the domain Ω.

4. The Navier–Stokes equations as a dynamical system

Before considering the dynamical behaviour of the Navier–Stokes equations using functional analysis tools, we need to define certain global flow quantities respectively known as the energy, enstrophy, and palinstrophy:

$$E = \frac{1}{2}|\boldsymbol{u}(t)|^2, \quad Z = \frac{1}{2}\left|A^{1/2}\boldsymbol{u}(t)\right|^2 = \frac{1}{2}||\boldsymbol{u}(t)||^2, \quad P = \frac{1}{2}|A\boldsymbol{u}(t)|^2.$$

Just as energy is proportional to the mean-squared velocity, enstrophy is proportional to the mean-squared vorticity and therefore provides a measure of the rotational energy in a flow. It is easily shown that the rate at which energy is dissipated is proportional to the enstrophy. Likewise, the enstrophy is dissipated at a rate proportional to the palinstrophy.

Taking the inner product of $\boldsymbol{u}$ (respectively $A\boldsymbol{u}$) with (7), we find

$$\frac{1}{2}\frac{d}{dt}|\boldsymbol{u}(t)|^2 + \nu||\boldsymbol{u}(t)||^2 = (\boldsymbol{f}, \boldsymbol{u}(t)), \tag{10}$$

$$\frac{1}{2}\frac{d}{dt}||\boldsymbol{u}(t)||^2 + \nu|A\boldsymbol{u}(t)|^2 = (\boldsymbol{f}, A\boldsymbol{u}(t)). \tag{11}$$

Applying the Cauchy–Schwarz and Poincaré inequalities, we obtain

$$(\boldsymbol{f}, \boldsymbol{u}(t)) \leq |\boldsymbol{f}||\boldsymbol{u}(t)|, \quad k_0^2|\boldsymbol{u}(t)|^2 \leq ||\boldsymbol{u}(t)||^2,$$

which leads to

$$-\nu||\boldsymbol{u}||^2 \leq -\nu k_0^2|\boldsymbol{u}|^2.$$

Thus, (10) can be written as

$$\frac{d}{dt}|\boldsymbol{u}(t)|^2 \leq -2\nu k_0^2|\boldsymbol{u}(t)|^2 + 2|\boldsymbol{f}|\,|\boldsymbol{u}(t)|. \tag{12}$$

Simplifying the above inequality yields

$$\frac{d}{dt}|\boldsymbol{u}(t)| \leq -\nu k_0^2|\boldsymbol{u}(t)| + |\boldsymbol{f}|, \tag{13}$$

which is a first-order differential inequality. If $\boldsymbol{f}$ is constant in time, we can apply a Gronwall inequality to (13) for $t \geq 0$:

$$|\boldsymbol{u}(t)| \leq e^{-\nu k_0^2 t}|\boldsymbol{u}(0)| + \left(\frac{1 - e^{-\nu k_0^2 t}}{\nu k_0^2}\right)|\boldsymbol{f}|. \tag{14}$$

Now, taking $\alpha \doteq e^{-\nu k_0^2 t}$ and $\beta \doteq |\boldsymbol{f}|/(\nu k_0^2)$, (14) can be expressed as

$$|\boldsymbol{u}(t)| \leq \alpha|\boldsymbol{u}(0)| + (1-\alpha)\beta,$$

which is a segment connecting $|\boldsymbol{u}(0)|$ and β. On squaring both sides and exploiting convexity, we obtain

$$|\boldsymbol{u}(t)|^2 \leq \alpha|\boldsymbol{u}(0)|^2 + (1-\alpha)\beta^2.$$

We thus arrive at the following result:

$$|\boldsymbol{u}(t)|^2 \leq e^{-\nu k_0^2 t}|\boldsymbol{u}(0)|^2 + (1-e^{-\nu k_0^2 t})\left(\frac{|\boldsymbol{f}|}{\nu k_0^2}\right)^2. \tag{15}$$

On introducing the Grashof number $G \doteq |\boldsymbol{f}|/(\nu^2 k_0^2)$, we simplify (15) to

$$|\boldsymbol{u}(t)|^2 \leq e^{-\nu k_0^2 t}|\boldsymbol{u}(0)|^2 + (1-e^{-\nu k_0^2 t})\nu^2 G^2. \tag{16}$$

Applying the same argument to (11), using (8), results in a similar estimate:

$$||\boldsymbol{u}(t)||^2 \leq e^{-\nu k_0^2 t}||\boldsymbol{u}(0)||^2 + (1-e^{-\nu k_0^2 t})\nu^2 k_0^2 G^2. \tag{17}$$

From (17), it can be observed that the closed ball $\mathfrak{B}$ of radius $\nu k_0 G$ in the space V is a bounded absorbing set [8], and so weakly compact.[1] If we take S to be the solution operator for (7) defined by

$$S(t)\boldsymbol{u}_0 = \boldsymbol{u}(t), \qquad \boldsymbol{u}_0 = \boldsymbol{u}(0) \in V,$$

where $\boldsymbol{u}(t)$ is the unique solution [11] of (7), then by the definition of the absorbing set for the solution of a dynamical system, for any bounded set $\mathfrak{B}' \subset V$, there exists a time t_0 such that

$$t_0 = t_0(\mathfrak{B}') \quad \text{and} \quad S(t)\mathfrak{B}' \subset \mathfrak{B}, \quad \forall t \geq t_0.$$

The global attractor $\mathcal{A}$ is then defined by

$$\mathcal{A} = \bigcap_{t \geq 0} S(t)\mathfrak{B}, \tag{18}$$

[1] Every closed and bounded convex set in a Hilbert space is compact in the weak topology.

so $\mathcal{A}$ is the largest bounded, invariant set such that $S(t)\mathcal{A} = \mathcal{A}$ for all $t \geq 0$. Taking into account in two dimensions the existence of a global attractor [16, 12] and a closed bounded absorbing set in $V \subset H$, an immediate observation from (16) and (17) shows that being on the attractor requires the following two conditions:

$$|\boldsymbol{u}| \leq \nu G, \tag{19a}$$

$$||\boldsymbol{u}|| \leq \nu k_0 G. \tag{19b}$$

The above observation leads to a suitable normalization for the energy and enstrophy that we use later on for finding bounds in the Z–E plane.

Remark. *The above results assure us that on the attractor both the energy and enstrophy are bounded.*

5. Relation between Z and E

Now that we have some useful estimates for enstrophy and energy, we can go further and find useful relations between Z and E. First, it is helpful to introduce a new quantity and a related theorem from Dascaliuc et al. [8], based on estimates detailed in Appendix A.5.

Definition. *For all $\boldsymbol{u} \in \mathcal{A}\backslash\{\mathbf{0}\}$, let*

$$\bar{\chi}(\boldsymbol{u}) = \frac{||\boldsymbol{u}||^2}{|\boldsymbol{u}|} = \frac{2Z}{\sqrt{2E}}.$$

Theorem 1. *The quotient $\bar{\chi}$ attains its absolute maximum on $\mathcal{A}\backslash\{\mathbf{0}\}$. Moreover, if $\mathbf{0} \in \mathcal{A}$, then*

$$\bar{\chi}(\boldsymbol{u}) \leq \nu^{2/3} k_0^2 G^{2/3} \Gamma_1^{1/3} |\boldsymbol{u}|^{1/3}, \quad \boldsymbol{u} \in \mathcal{A}\backslash\{\mathbf{0}\},$$

where $\Gamma_1 = 2(\Lambda_2^{1/2}\Gamma_0^{1/2} + 2c_L^2 G^2 \Gamma_0)$, $\Gamma_0 = c_L^2 G^2 + 2\Lambda_1^{1/2}$, and $\Lambda_j = \dfrac{\left|A^{j/2}\boldsymbol{f}\right|^2}{k_0^{2j}|\boldsymbol{f}|^2}$.

Proof. *See Dascaliuc et al. [8, Theorem 5.1].* ∎

Remark. *Let $\boldsymbol{u}(t)$ be a solution such that $\boldsymbol{u}(t) \neq 0$ on some interval $(t_1, t_2]$. Then the function $\chi(t) \doteq \bar{\chi}(\boldsymbol{u}(t)) = ||\boldsymbol{u}(t)||^2/|\boldsymbol{u}(t)|$ satisfies*

$$\frac{d\chi}{dt} = \frac{\dfrac{d||\boldsymbol{u}||^2}{dt}|\boldsymbol{u}| - ||\boldsymbol{u}||^2 \dfrac{d|\boldsymbol{u}|}{dt}}{|\boldsymbol{u}|^2} = \frac{2\left[(\boldsymbol{f}, A\boldsymbol{u}) - \nu|A\boldsymbol{u}|^2\right]}{|\boldsymbol{u}|} - \frac{||\boldsymbol{u}||^2[(\boldsymbol{f}, \boldsymbol{u}) - \nu||\boldsymbol{u}||^2]}{|\boldsymbol{u}|^3}. \tag{20}$$

Using the definition

$$\lambda = \lambda(t) = \frac{\chi(t)}{|\boldsymbol{u}(t)|} = \frac{||\boldsymbol{u}(t)||^2}{|\boldsymbol{u}(t)|^2},$$

we can rewrite (20) as

$$|\boldsymbol{u}|\frac{d\chi}{dt} = -2\nu|(A-\lambda)\boldsymbol{u}|^2 + 2(\boldsymbol{f},(A-\lambda)\boldsymbol{u}) + \lambda(\boldsymbol{f},\boldsymbol{u}) - \nu\lambda^2|\boldsymbol{u}|^2. \tag{21}$$

By introducing

$$\boldsymbol{f}^\perp = \boldsymbol{f} - \frac{(\boldsymbol{f},\boldsymbol{u})\boldsymbol{u}}{|\boldsymbol{u}|^2},$$

it is observed that

$$\begin{aligned}
(\boldsymbol{f},(\boldsymbol{A}-\lambda)\boldsymbol{u}) - \left(\boldsymbol{f}^\perp,(\boldsymbol{A}-\lambda)\boldsymbol{u}\right) &= \left(\frac{(\boldsymbol{f},\boldsymbol{u})}{|\boldsymbol{u}|^2}\boldsymbol{u},(\boldsymbol{A}-\lambda)\boldsymbol{u}\right)\\
&= \frac{(\boldsymbol{f},\boldsymbol{u})}{|\boldsymbol{u}|^2}[(\boldsymbol{u},\boldsymbol{A}\boldsymbol{u}) - (\boldsymbol{u},\lambda\boldsymbol{u})]\\
&= \frac{(\boldsymbol{f},\boldsymbol{u})}{|\boldsymbol{u}|^2}\left(||\boldsymbol{u}||^2 - \lambda|\boldsymbol{u}|^2\right) = 0.
\end{aligned}$$

Thus (21) can be rewritten as

$$\begin{aligned}
|\boldsymbol{u}|\frac{d\chi}{dt} &= -2\nu|(A-\lambda)\boldsymbol{u}|^2 + 2(\boldsymbol{f}^\perp,(A-\lambda)\boldsymbol{u}) + \lambda(\boldsymbol{f},\boldsymbol{u}) - \nu\lambda^2|\boldsymbol{u}|^2\\
&= -2\nu\left|(A-\lambda)\boldsymbol{u} - \frac{\boldsymbol{f}^\perp}{2\nu}\right|^2 + \frac{\left|\boldsymbol{f}^\perp\right|^2}{2\nu} + \lambda(\boldsymbol{f},\boldsymbol{u}) - \nu\lambda^2|\boldsymbol{u}|^2.
\end{aligned} \tag{22}$$

On defining

$$\boldsymbol{v} = (A-\lambda)\boldsymbol{u} - \frac{\boldsymbol{f}^\perp}{2\nu}, \qquad \sigma = \frac{(\boldsymbol{f},\boldsymbol{u})}{|\boldsymbol{f}||\boldsymbol{u}|},$$

we can represent (22) as

$$|\boldsymbol{u}|\frac{d\chi}{dt} = -2\nu|\boldsymbol{v}|^2 + \frac{|\boldsymbol{f}|^2}{2\nu}(1-\sigma^2) - \nu\chi^2 + \chi\sigma|\boldsymbol{f}|,$$

so that

$$
\begin{aligned}
|\boldsymbol{u}|\frac{d}{dt}\left(\frac{|\boldsymbol{f}|}{\nu}-\chi\right) &= 2\nu|\boldsymbol{v}|^2+\nu\chi^2-\frac{|\boldsymbol{f}|^2}{2\nu}(1-\sigma^2)-\chi\sigma|\boldsymbol{f}| \\
&= 2\nu|\boldsymbol{v}|^2+\nu\left(\frac{|\boldsymbol{f}|}{\nu}-\chi\right)^2-\frac{|\boldsymbol{f}|^2}{\nu}+2\chi|\boldsymbol{f}|-\frac{|\boldsymbol{f}|^2}{2\nu}(1-\sigma^2)-\chi\sigma|\boldsymbol{f}| \\
&= 2\nu|\boldsymbol{v}|^2+\nu\left(\frac{|\boldsymbol{f}|}{\nu}-\chi\right)^2-(2-\sigma)|\boldsymbol{f}|\left(\frac{|\boldsymbol{f}|}{\nu}-\chi\right) \\
&\quad +(2-\sigma)\frac{|\boldsymbol{f}|^2}{\nu}-(3-\sigma^2)\frac{|\boldsymbol{f}|^2}{2\nu} \\
&= 2\nu|\boldsymbol{v}|^2+\nu\left(\frac{|\boldsymbol{f}|}{\nu}-\chi\right)^2-(2-\sigma)|\boldsymbol{f}|\left(\frac{|\boldsymbol{f}|}{\nu}-\chi\right)+(1-\sigma)^2\frac{|\boldsymbol{f}|^2}{2\nu}.
\end{aligned}
$$

Again, introducing

$$
\begin{aligned}
\phi &= 2\nu|\boldsymbol{v}|^2+\nu\left(\frac{|\boldsymbol{f}|}{\nu}-\chi\right)^2+(1-\sigma)^2\frac{|\boldsymbol{f}|^2}{2\nu}\geq 0, \\
\psi &= (2-\sigma)|\boldsymbol{f}|\geq|\boldsymbol{f}|
\end{aligned}
\tag{23}
$$

results in

$$
\frac{d}{dt}\left(\frac{|\boldsymbol{f}|}{\nu}-\chi\right)=\frac{\phi}{|\boldsymbol{u}|}-\frac{\psi}{|\boldsymbol{u}|}\left(\frac{|\boldsymbol{f}|}{\nu}-\chi\right),
$$

whose solution can be easily obtained for $t_0\leq t,\ t,t_0\in(t_1,t_2]$*:*

$$
\frac{|\boldsymbol{f}|}{\nu}-\chi=\left(\frac{|\boldsymbol{f}|}{\nu}-\chi(t_0)\right)\exp\left(-\int_{t_0}^{t}\frac{\psi}{|\boldsymbol{u}|}\,dt\right)+\int_{t_0}^{t}\frac{\phi}{|\boldsymbol{u}|}\exp\left(-\int_{\tau}^{t}\frac{\psi}{|\boldsymbol{u}|}\,dt\right)d\tau.
\tag{24}
$$

6. Bounds in the Z–E plane

In this section we present bounds on the attractor in the Z–E plane using some functional inequalities and the dynamical behaviour of the Navier–Stokes equations presented in the previous section. One useful and important bound is obtained from the Poincaré inequality:

$$
k_0^2|\boldsymbol{u}|^2\leq||\boldsymbol{u}||^2\quad\Rightarrow\quad k_0^2E\leq Z.
\tag{25}
$$

As we have observed, the above inequality will impose a lower bound on the attractor in the Z–E plane. A less trivial upper bound relies on the following key theorem from Dascaliuc et al. [8].

Theorem 2. *For all $\boldsymbol{u} \in \mathcal{A}$,*

$$||\boldsymbol{u}||^2 \leq \frac{|\boldsymbol{f}|}{\nu}|\boldsymbol{u}|. \tag{26}$$

In the case $||\boldsymbol{u}_0||^2 = \dfrac{|\boldsymbol{f}|}{\nu}|\boldsymbol{u}_0|$ for $\boldsymbol{u}_0 \in \mathcal{A}\backslash\{\mathbf{0}\}$, it follows that $\boldsymbol{u}_0$ is a stationary solution and there exists $n_0 \in \mathbb{N}$ such that $\boldsymbol{f} = R_{n_0}\boldsymbol{f}$ and $\boldsymbol{u}_0 = \dfrac{\boldsymbol{f}}{\nu\lambda_{n_0}}$. Moreover, in this case $\mathbf{0} \notin \mathcal{A}$ and for all $\boldsymbol{u} \in \mathcal{A}\backslash\{\boldsymbol{u}_0\}$

$$||\boldsymbol{u}||^2 \leq \lambda_{n_0}|\boldsymbol{u}|^2, \quad ||\boldsymbol{u}||^2 \leq \frac{|\boldsymbol{f}|}{\nu}|\boldsymbol{u}| = G\nu\lambda_0|\boldsymbol{u}|. \tag{27}$$

Proof. *Here we will just present the proof of (26), which is needed in the following section; for the remaining parts of the theorem, the reader is referred to Dascaliuc et al. [8, Theorem 5.2]. Let $\boldsymbol{u}_0 \in \mathcal{A}$. If $\boldsymbol{u}_0 = \mathbf{0}$, then it is clear that (26) holds. Now if $\boldsymbol{u}_0 \neq \mathbf{0}$, let $\boldsymbol{u}(t)$ be the solution for $\boldsymbol{u}(0) = \boldsymbol{u}_0$. There are two cases to consider:*

- ***Case 1***
  Suppose that we have $\inf_{t\in(-\infty,0]} |\boldsymbol{u}(t)| = u' > 0$. This together with the boundedness of enstrophy (19b) implies that χ is bounded. Also, from (19a) and (23) we obtain

  $$\lim_{t_0\to-\infty} \exp\left(-\int_\tau^t \frac{\psi}{|\boldsymbol{u}|}\,dt\right) \leq \lim_{t_0\to-\infty} \exp\left(-\frac{|\boldsymbol{f}|}{\nu G}(t-t_0)\right) = 0.$$

  Now if we take $t = 0$ and $t_0 \to -\infty$, then (24) results in $|\boldsymbol{f}|/\nu - \chi(0) \geq 0$. Then (24) will immediately yield $|\boldsymbol{f}|/\nu - \chi(t) \geq 0$, and thus (26) holds.

- ***Case 2***
  Suppose that $\inf_{t\in(-\infty,0]} |\boldsymbol{u}(t)| = 0$. Then there exists a $t_0 < 0$ such that

  $$|\boldsymbol{u}(t_0)|^{1/3} \leq \frac{|\boldsymbol{f}|}{\nu^{5/3}k_0^2G^{2/3}\Gamma_1^{1/3}},$$

  where Γ_1 is defined in Theorem 1. Since $\mathbf{0} \in \mathcal{A}$ ($\mathcal{A}$ is weakly compact), we can apply Theorem 1 to find

  $$\frac{|\boldsymbol{f}|}{\nu} - \chi(t_0) \geq 0, \quad \forall t \geq t_0.$$

Thus, by the last part of the proof given for ***case 1****, (26) follows and hence for all* $\boldsymbol{u} \in \mathcal{A}$*, we have*

$$||\boldsymbol{u}||^2 \leq \frac{|\boldsymbol{f}|}{\nu}|\boldsymbol{u}|.$$

■

Then, if we define $\boldsymbol{v}(t) = \dfrac{\boldsymbol{u}(t)}{\nu G}$, we see that (26) simplifies to

$$||\boldsymbol{v}||^2 \leq k_0^2|\boldsymbol{v}|. \tag{28}$$

For constant forcing the projection of the global attractor is thus located inside the bounded region shown in Figure 1. A low-resolution attempt to numerically illustrate these bounds can be found for banded forcing in Ref. [6]. Another low-resolution study in Ref. [10] examined forcing at a single eigenmode of the Stokes operator (which we point out cannot generate a turbulent spectrum from zero initial conditions).

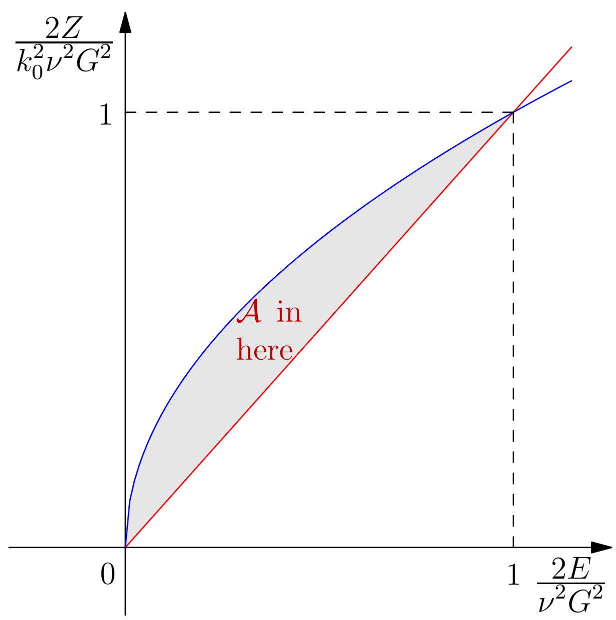

Figure 1: Bounds in the Z–E plane

7. Energy and Enstrophy Relations on the Global Attractor of the 2D Navier–Stokes Equations: Random Forcing

In this section we are going to extend our analysis to random forcing, which provides a more realistic way of injecting energy into a turbulent system than constant forcing. One of the important types of random forcing, called white-noise forcing, can be readily implemented numerically, an advantage that we will exploit in Section 10.

Generalizing the previous analysis to account for random forcing requires a new norm that combines the L^2 norm from the previous section with an ensemble average:

$$|\boldsymbol{f}|_{\tilde{\omega}} \doteq \left(\int_{\Omega} \left\langle |\boldsymbol{f}|_{L^2}^2 \right\rangle \, d\boldsymbol{x} \right)^{1/2},$$

where $\tilde{\omega}$ indicates that this norm applies to a real-valued random variable. For a random variable α, with probability density function P, we define the ensemble average $\langle \alpha \rangle = \int_{-\infty}^{\infty} \alpha (dP/d\zeta) \, d\zeta$. As we want to define our problem in a Hilbert space, to exploit the properties of the Stokes operator A, the above norm must come from an inner product on that Hilbert space. So although the above definition defines a norm, the essential point in extending our analysis is defining a suitable inner product on the Hilbert space H of random-valued functions.

7.1. Extended inner-product for random-valued functions in H

As an extension of the inner product we applied in the previous section, let us define

$$(\boldsymbol{u}, \boldsymbol{v})_{\tilde{\omega}} \doteq \int_{\Omega} \langle \boldsymbol{u} \cdot \boldsymbol{v} \rangle \, d\boldsymbol{x} = \int_{\Omega} \left(\int_{-\infty}^{\infty} \boldsymbol{u} \cdot \boldsymbol{v} \, \frac{dP}{d\zeta} d\zeta \right) d\boldsymbol{x}.$$

Adopting the above extended inner product, the definitions of energy, enstrophy, and palinstrophy are unchanged, consistent with our previous analysis. From here on, for simplicity we will denote $|\cdot|_{\tilde{\omega}}$ by $|\cdot|$ and $(\boldsymbol{u}, \boldsymbol{v})_{\tilde{\omega}}$ by $(\boldsymbol{u}, \boldsymbol{v})$.

8. The Navier–Stokes equations with random forcing as a dynamical system

The energy evolves according to

$$\frac{1}{2} \frac{d}{dt} |\boldsymbol{u}|^2 + \nu (A\boldsymbol{u}, \boldsymbol{u}) + (\mathcal{B}(\boldsymbol{u}, \boldsymbol{u}), \boldsymbol{u}) = (\boldsymbol{f}, \boldsymbol{u}).$$

Since $(\mathcal{B}(\boldsymbol{u},\boldsymbol{u}),\boldsymbol{u}) = 0$, we obtain

$$\frac{1}{2}\frac{d}{dt}|\boldsymbol{u}|^2 + \nu\left|A^{1/2}\boldsymbol{u}\right|^2 = \epsilon,$$

where $\epsilon = (\boldsymbol{f},\boldsymbol{u})$ is the energy injection rate. Equivalently,

$$\frac{1}{2}\frac{d}{dt}|\boldsymbol{u}|^2 + \nu||\boldsymbol{u}||^2 = \epsilon.$$

The Poincaré inequality then yields

$$\frac{1}{2}\frac{d}{dt}|\boldsymbol{u}|^2 \le \epsilon - \nu k_0^2|\boldsymbol{u}|^2 \overset{\text{Gronwall inequality}}{\Rightarrow}$$
$$|\boldsymbol{u}(t)|^2 \le e^{-2\nu k_0^2 t}|\boldsymbol{u}(0)|^2 + \left(\frac{1-e^{-2\nu k_0^2 t}}{\nu k_0^2}\right)\epsilon.$$

So for every $\boldsymbol{u} \in \mathcal{A}$, where $\mathcal{A}$ is a random (pullback) attractor [5], we would expect to have

$$|\boldsymbol{u}(t)|^2 \le \frac{\epsilon}{\nu k_0^2}. \tag{29}$$

Similarly, from the enstrophy equation

$$\frac{1}{2}\frac{d}{dt}\left|A^{1/2}\boldsymbol{u}\right|^2 + \nu(A^{1/2}\boldsymbol{u}, A^{3/2}\boldsymbol{u}) + (\mathcal{B}(\boldsymbol{u},\boldsymbol{u}), A\boldsymbol{u}) = (A^{1/2}\boldsymbol{f}, A^{1/2}\boldsymbol{u}),$$

we obtain

$$\frac{1}{2}\frac{d}{dt}||\boldsymbol{u}||^2 + \nu|A\boldsymbol{u}|^2 = \eta,$$

where $\eta = (\boldsymbol{f}, A\boldsymbol{u})$ is the enstrophy injection rate. Again with the help of the Poincaré inequality we find

$$\frac{1}{2}\frac{d}{dt}||\boldsymbol{u}||^2 \le \eta - \nu k_0^2||\boldsymbol{u}||^2 \overset{\text{Gronwall inequality}}{\Rightarrow}$$
$$||\boldsymbol{u}(t)||^2 \le e^{-2\nu k_0^2 t}||\boldsymbol{u}(0)||^2 + \left(\frac{1-e^{-2\nu k_0^2 t}}{\nu k_0^2}\right)\eta,$$

from which we deduce that $||\boldsymbol{u}(t)||^2 \le \eta/(\nu k_0^2)$ for every $\boldsymbol{u} \in \mathcal{A}$.

113 ## 9. An upper bound in the Z–E plane for a random forcing

Let $\boldsymbol{u}(t)$ be a solution such that $\boldsymbol{u}(t) \neq 0$ on some interval $(t_1, t_2]$. Then the function $\chi(t) = ||\boldsymbol{u}(t)||^2/|\boldsymbol{u}(t)|$ satisfies (20), with the norms now based on our extended inner product. Using the definition

$$\lambda = \lambda(t) = \frac{\chi(t)}{|\boldsymbol{u}|} = \frac{||\boldsymbol{u}||^2}{|\boldsymbol{u}|^2},$$

114 we see that (20) can be written as

$$|\boldsymbol{u}|\frac{d\chi}{dt} = -2\nu|A\boldsymbol{u}|^2 + 2(\boldsymbol{f}, A\boldsymbol{u}) - \lambda(\boldsymbol{f}, \boldsymbol{u}) + \underbrace{\nu\lambda||\boldsymbol{u}||^2}_{\nu\lambda^2|\boldsymbol{u}|^2}. \tag{30}$$

On introducing $\boldsymbol{v} = (A - \lambda)\boldsymbol{u} - \dfrac{\boldsymbol{f}}{2\nu}$, then

$$\begin{aligned} -2\nu|\boldsymbol{v}|^2 &= -2\nu|A\boldsymbol{u}|^2 + 2(\boldsymbol{f}, A\boldsymbol{u}) - 2\lambda(\boldsymbol{f}, \boldsymbol{u}) + 4\nu\lambda||\boldsymbol{u}||^2 - 2\nu\lambda^2|\boldsymbol{u}|^2 - \frac{|\boldsymbol{f}|^2}{2\nu} \\ &= |\boldsymbol{u}|\frac{d\chi}{dt} - \lambda(\boldsymbol{f}, \boldsymbol{u}) + \nu\chi^2 - \frac{|\boldsymbol{f}|^2}{2\nu} = |\boldsymbol{u}|\frac{d\chi}{dt} - \frac{\epsilon}{|\boldsymbol{u}|}\chi + \nu\chi^2 - \frac{|\boldsymbol{f}|^2}{2\nu}. \end{aligned}$$

On introducing a real constant α to be determined later, we may write

$$|\boldsymbol{u}|\frac{d}{dt}(\alpha - \chi) = 2\nu|\boldsymbol{v}|^2 + \nu(\alpha - \chi)^2 - \nu\alpha^2 + \left(2\nu\alpha - \frac{\epsilon}{|\boldsymbol{u}|}\right)\chi - \frac{|\boldsymbol{f}|^2}{2\nu}.$$

The above result can be rewritten in the following form

$$|\boldsymbol{u}|\frac{d}{dt}(\alpha - \chi) = 2\nu|\boldsymbol{v}|^2 + \nu(\alpha - \chi)^2 - \beta(\alpha - \chi) + \nu\alpha^2 - \frac{\epsilon}{|\boldsymbol{u}|}\alpha - \frac{|\boldsymbol{f}|^2}{2\nu},$$

where $\beta \doteq 2\nu\alpha - \dfrac{\epsilon}{|\boldsymbol{u}|}$. Thus, if α is such that

$$\beta = 2\nu\alpha - \frac{\epsilon}{|\boldsymbol{u}|} > 0 \quad \text{and} \quad \nu\alpha^2 - \frac{\epsilon\alpha}{|\boldsymbol{u}|} - \frac{|\boldsymbol{f}|^2}{2\nu} > 0, \tag{31}$$

we can introduce

$$\phi \doteq 2\nu|\boldsymbol{v}|^2 + \nu(\alpha - \chi)^2 + \nu\alpha^2 - \frac{\epsilon}{|\boldsymbol{u}|}\alpha - \frac{|\boldsymbol{f}|^2}{2\nu} > 0$$

to express the above first-order differential equation as

$$|\boldsymbol{u}|\frac{d}{dt}(\alpha-\chi)+\beta(\alpha-\chi)=\phi. \tag{32}$$

The solution to this equation is

$$\alpha-\chi(t)=(\alpha-\chi(t_0))\exp\left(-\int_{t_0}^{t}\frac{\beta}{|\boldsymbol{u}|}\,dt\right)+\int_{t_0}^{t}\frac{\phi}{|\boldsymbol{u}|}\exp\left(-\int_{\tau}^{t}\frac{\beta}{|\boldsymbol{u}|}\,dt\right)d\tau.$$

Taking $t_0\to-\infty$ and $t=0$ results in $\alpha-\chi(0)\geq 0$. Now taking $t_0=0$, and $t\to\infty$, one finds that $\alpha-\chi(t)\geq 0$ for all $t\in(-\infty,\infty)$. That is,

$$||\boldsymbol{u}||^2\leq\alpha|\boldsymbol{u}|. \tag{33}$$

To obtain the above result we need to check conditions (31). Working on these inequalities, one can show

$$\nu\alpha^2-\frac{\epsilon\alpha}{|\boldsymbol{u}|}-\frac{|\boldsymbol{f}|^2}{2\nu}=0\Rightarrow\alpha_{+,-}=\frac{\dfrac{\epsilon}{|\boldsymbol{u}|}\pm\sqrt{\dfrac{\epsilon^2}{|\boldsymbol{u}|^2}+2|\boldsymbol{f}|^2}}{2\nu}\Rightarrow\begin{cases}\alpha_-<0,\\ \alpha_+\geq\dfrac{\epsilon}{\nu|\boldsymbol{u}|}.\end{cases}$$

Thus

$$\nu\alpha^2-\frac{\epsilon\alpha}{|\boldsymbol{u}|}-\frac{|\boldsymbol{f}|^2}{2\nu}>0\iff\alpha\geq\frac{\epsilon}{\nu|\boldsymbol{u}|}\text{ or }\alpha\leq\alpha_-<0.$$

For $\alpha\geq\dfrac{\epsilon}{\nu|\boldsymbol{u}|}$, we see that $\beta=2\nu\alpha-\dfrac{\epsilon}{|\boldsymbol{u}|}>0$. Moreover, from (29), we see that $\dfrac{\epsilon}{\nu|\boldsymbol{u}|}\geq k_0\sqrt{\dfrac{\epsilon}{\nu}}$. So if we take $\alpha=k_0\sqrt{\dfrac{\epsilon}{\nu}}$, then (33) gives us an upper bound for enstrophy in the Z–E plane:

$$||\boldsymbol{u}||^2\leq k_0\sqrt{\frac{\epsilon}{\nu}}|\boldsymbol{u}|. \tag{34}$$

We have thus proved the following theorem.

Theorem 3. *For all $\boldsymbol{u}\in\mathcal{A}$ driven by a random forcing injecting energy at a rate ϵ,*

$$||\boldsymbol{u}||^2\leq k_0\sqrt{\frac{\epsilon}{\nu}}\,|\boldsymbol{u}|.$$

We note that (29) and the Cauchy–Schwarz inequality lead to the following lower bound for $|\boldsymbol{f}|$:

$$k_0\sqrt{\nu\epsilon} \le \frac{\epsilon}{|\boldsymbol{u}|} = \frac{(\boldsymbol{f},\boldsymbol{u})}{|\boldsymbol{u}|} \le \frac{|\boldsymbol{f}||\boldsymbol{u}|}{|\boldsymbol{u}|} = |\boldsymbol{f}|. \tag{35}$$

It is convenient to use this lower bound for $|\boldsymbol{f}|$ to define a lower bound for a modified Grashof number $G_* = |\boldsymbol{f}|_{\mathsf{T}\omega}/(\nu^2 k_0^2)$, which we adopt as the normalization $\tilde{G}$ for random forcing:

$$\tilde{G} = \frac{1}{k_0}\sqrt{\frac{\epsilon}{\nu^3}}.$$

Then, if we define $\boldsymbol{v}(t) = \dfrac{\boldsymbol{u}(t)}{\nu\tilde{G}}$, we see that (34) simplifies to

$$||\boldsymbol{v}||^2 \le k_0^2|\boldsymbol{v}|. \tag{36}$$

We observe that this normalized bound has the same form as the upper bound (28) found by Dascaliuc et al. [7, Theorem 4.1] for constant forcing, thus elucidating the relation between these two types of forcing.

10. Numerical Simulations

In this section we report on the results of pseudospectral simulations of 2D incompressible homogeneous isotropic turbulence with white-noise forcing and periodic boundary conditions, performed with a state-of-the-art direct numerical simulation (DNS) code, publicly available at https://github.com/dealias/dns. We recall that one of the main assumptions behind almost all theoretical analysis of incompressible homogeneous isotropic turbulence is that the Reynolds number R_e is very large. Direct numerical simulation of high-Reynolds turbulence is computationally very expensive (unless either the simulation domain is small or a heuristic subgrid scale model is employed). This requires an extremely refined grid and an enormous number of time steps, both of which are obstacles towards numerically simulating turbulence. The reader must therefore bear in mind that simulations based on the DNS method are just rough approximations of high-Reynolds number flows, full realizations of which will likely remain infeasible until at least the mid-21st century.

10.1. An overview of the 2D **DNS** *code*

The 2D DNS code, written in C++, is comprised of a kernel called TRIAD built around an advanced adaptive integrator for discretized initial value problems. This package provides several different numerical integration schemes that can be selected by the user at run time. The DNS module provides TRIAD with an advanced pseudospectral solver that uses the FFTW++ library [4] for calculating implicitly dealiased convolutions, exploiting Hermitian symmetry [3, 18]. Advanced computer memory management, such as implicit padding, memory alignment, and dynamic moment averaging allow DNS to attain its extreme performance. It uses the formulation proposed by Basdevant [1] (discussed in Appendix C) to reduce the number of FFTs required for 2D (3D) incompressible turbulence to four (eight). The reader who is interested in learning more about the DNS code is referred to https://github.com/dealias/dns/tree/master/2d. Simplified 2D and 3D versions called PROTODNS have also been developed for educational purposes: https://github.com/dealias/dns/tree/master/protodns.

10.2. Numerical implementation

Before presenting the simulations, it is vital to talk briefly about some numerical considerations. The 2D variant of the Kolmogorov theory proposed by Kraichnan [15], Leith [17], and Batchelor [2] involves both a direct cascade of enstrophy and an inverse cascade of energy. This means that energy is transferred to low wavenumbers (large scales), where it eventually piles up. In nature, 2D turbulence is believed to occur under special circumstances in high altitude layers of the atmosphere. In this case, the energy cascading to the large scales is taken out by some external physical mechanism like atmospheric gravity waves. Many researchers model such processes by adding an artificial damping to the Navier–Stokes equations. Although there are different approaches toward applying such a *hypoviscosity*, such as a large-scale friction, such methods change the governing equations: one does not actually solve the pure Navier–Stokes equations when these energy extracting mechanisms are implemented.

Although the DNS code has the capability of solving the pure Navier–Stokes equations, it can optionally apply a large-scale linear friction term proportional to the velocity, with a coefficient ν_L, in analogy with the molecular viscosity term, with a coefficient ν_H. We have numerically investigated the effect of this hypoviscosity on the global attractor, an investigation that has not previously been performed and that opens up new avenues in the debate about the possible effects of such artificial energy damping methods. In the following numerical results, the choice $\nu_L = 0$ indicates the solution of the pure Navier–Stokes equations (truncated at a high wavenumber, corresponding to the given resolution).

We evolve the two-dimensional forced-dissipative equation for the scalar *vorticity* $\omega = \hat{\boldsymbol{z}}\boldsymbol{\cdot}\boldsymbol{\nabla}\times\boldsymbol{u}$:

$$\frac{\partial\omega}{\partial t} + (\hat{\boldsymbol{z}}\times\boldsymbol{\nabla}\nabla^{-2}\omega\boldsymbol{\cdot}\boldsymbol{\nabla})\omega = \nu_H\nabla^2\omega + f, \tag{37}$$

where $\hat{\boldsymbol{z}}$ is the unit normal to the flow plane. Upon Fourier transforming and adding an optional large-scale hypoviscosity (friction) term $-H(k_L - k)\nu_L\omega_{\boldsymbol{k}}$, where H is the Heaviside unit step function and k_L is a large-scale hypoviscosity threshold, we obtain an equation of the form

$$\frac{\partial\omega_{\boldsymbol{k}}}{\partial t} = S_{\boldsymbol{k}} - \nu_H k^2\omega_{\boldsymbol{k}} - \nu_L H(k_L - k)\omega_{\boldsymbol{k}} + f_{\boldsymbol{k}}, \tag{38}$$

where $S_{\boldsymbol{k}} = \sum_{\boldsymbol{q}} \hat{\boldsymbol{z}}\boldsymbol{\cdot}\boldsymbol{k}\times\boldsymbol{q}\,\omega_{\boldsymbol{k}-\boldsymbol{q}}\omega_{\boldsymbol{q}}/q^2$ represents the advective convolution. The enstrophy spectrum $Z(k) = k^2E(k)$ is then seen to satisfy a balance equation of the form

$$\frac{\partial}{\partial t}Z(k) + 2[\nu_H k^2 + \nu_L H(k_L - k)]Z(k) = 2T(k) + G(k), \tag{39}$$

where $T(k)$ and $G(k)$ represent angular sums of $\mathrm{Re}\,\langle S_{\boldsymbol{k}}\overline{\omega}_{\boldsymbol{k}}\rangle$ and $\mathrm{Re}\,\langle f_{\boldsymbol{k}}\overline{\omega}_{\boldsymbol{k}}\rangle$, respectively. Following Kraichnan [14], it is convenient to define the nonlinear enstrophy transfer $\Pi(k) = 2\int_k^\infty T(p)\,dp$, which measures the cumulative nonlinear transfer of enstrophy into $[k,\infty)$. On integrating (39) from k to ∞, we find

$$\frac{d}{dt}\int_k^\infty Z(p)\,dp = \Pi(k) - \eta(k),$$

where $\eta(k) \doteq 2\int_k^\infty[\nu_H p^2 + \nu_L H(k_L - k)]Z(p)\,dp - \int_k^\infty G(p)\,dp$ is the total enstrophy transfer, via dissipation and forcing, out of wavenumbers higher than k. A positive (negative) value for $\Pi(k)$ represents a flow of enstrophy to wavenumbers higher (lower) than k. When $\nu_H = f = 0$, enstrophy conservation implies that

$$0 = \frac{d}{dt}\int_0^\infty Z(p)\,dp = 2\int_0^\infty T(p)\,dp,$$

so that

$$\Pi(k) = 2\int_k^\infty T(p)\,dp = -2\int_0^k T(p)\,dp. \tag{40}$$

We note that $\Pi(0) = \Pi(\infty) = 0$. Moreover, in a statistically steady state $\Pi(k) = \eta(k)$; this provides an excellent numerical diagnostic for validating a steady state.

We evolve the simulations starting from the anisotropic Hermitian initial condition

$$\boldsymbol{\omega}_0(k_x, k_y) = \frac{\sqrt{k_x^2 + k_y^2} + i(k_x + k_y)}{\sqrt{\alpha + \beta(k_x^2 + k_y^2)}},$$

which corresponds to an initial energy spectrum $E(k) = \pi k/(\alpha + \beta k^2)$ and total energy $E = \int E(k)\,dk = \frac{1}{2}\sum_{\boldsymbol{k}} \omega_{\boldsymbol{k}}^2/k^2$. The turbulence is driven by a white-noise forcing limited to an annulus of mean radius k_f and width δ_f in Fourier space. The energy injection rate ϵ is measured by averaging the spectral contributions from the random forcing:

$$\epsilon = \sum_{\boldsymbol{k}} \frac{\langle f_{\boldsymbol{k}}, \omega_{\boldsymbol{k}} \rangle}{k^2}.$$

As is usual in numerical simulations of turbulence, we assume that the ergodic theorem is sufficiently applicable so that ensemble averages may be approximated by temporal averages. For convenience, we take $L = 2\pi$, so that $k_0 = 1$.

10.3. Numerical results

In Figures 2 and 3 the vorticity fields are shown for two numerical simulations of (37) with identical values of η, k_f, δ_f, α, β, and ν_H, but different values of ν_L. Figure 2 demonstrates the effect of applying an artificial energy damping mechanism at large scales, with $\nu_L = 0.15$ and $k_L = 3.5$, whereas Figure 3 depicts the vorticity field for the pure Navier–Stokes equations considered in the theoretical analysis of this work, where $\nu_L = 0$. Figures 4 and 5 illustrate the Z–E evolution for these simulations, respectively. Each dot, colored using a rainbow palette (violet to red) to represent relative time, corresponds to 1000 variable time steps of mean duration 0.003 and 0.0005, respectively. Comparing these results highlights the dramatic impact that the hypoviscosity term $-H(k_L - k)\nu_L\omega$ in (38) has on the turbulent dynamics. Instead of approaching the projected global attractor that we have found for (7), the solutions are absorbed into the region characterized by the two pink lines in Figure 4 that denote the slopes $k_f + \delta_f/2$ and $k_f - \delta_f/2$, respectively. In contrast, once the hypoviscous term is removed, we observe in Fig. 5 excellent agreement of the numerical simulation and the predicted projection of the global attractor on the Z–E plane. The grey line represents (25) and the brown line represents (36).

Figures 6 and 7 demonstrate the energy spectrums corresponding to these simulations. As is seen in Figure 6, the application of an energy damping mechanism at large scales tends to flatten the large-scale energy spectrum, while in Figure 7, the absence of this mechanism is reflected as a steeper slope for the energy spectrum at large scales. Figures 8 and 9 represent the energy and enstrophy transfers for the corresponding simulations. The coincidence of these graphs (which is expected theoretically) is an indication of being in a quasisteady state, where both the enstrophy injection and dissipation rates are nearly in balance.

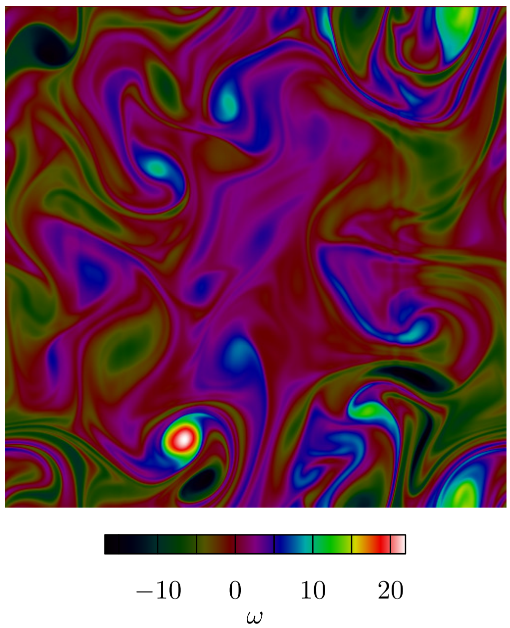

Figure 2: Vorticity field at $t = 1650$ for white-noise forcing computed with 511×511 dealiased modes using $\eta = 1$, $k_f = 4$, $\delta_f = 1$, $k_L = 3.5$, $\nu_H = 0.0005$, $\nu_L = 0.15$, $\alpha = 10^4$, and $\beta = 10^4$.

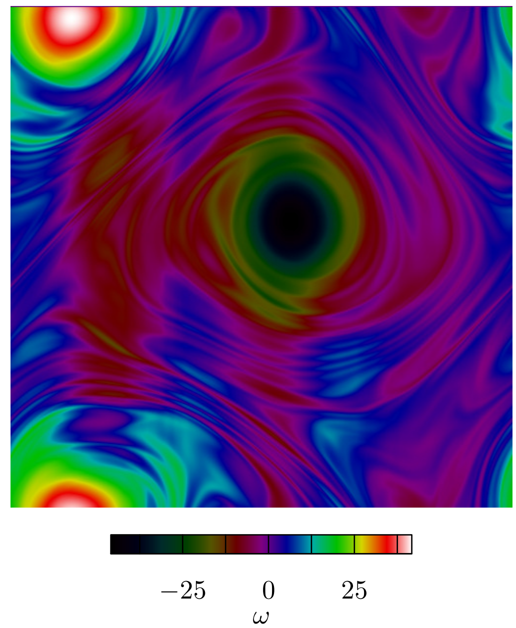

Figure 3: Vorticity field at $t = 1650$ for white-noise forcing computed with 511×511 dealiased modes using $\eta = 1$, $k_f = 4$, $\delta_f = 1$, $\nu_H = 0.0005$, $\nu_L = 0$, $\alpha = 10^4$, and $\beta = 10^4$.

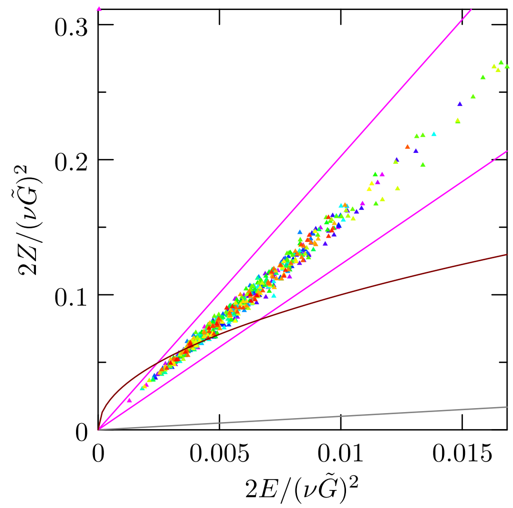

Figure 4: Enstrophy vs. energy evolution for the simulation shown in Fig. 2.

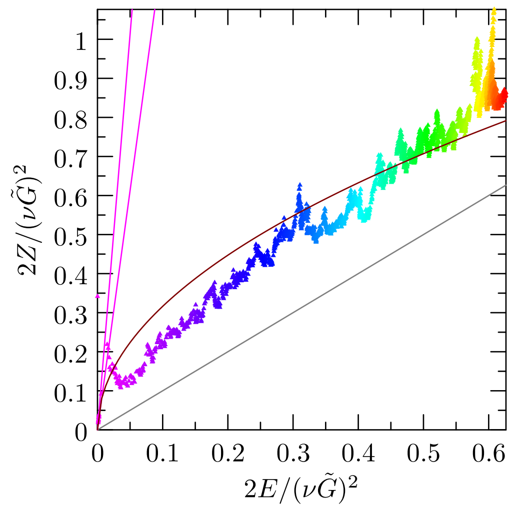

Figure 5: Enstrophy vs. energy evolution for the simulation shown in Fig. 3.

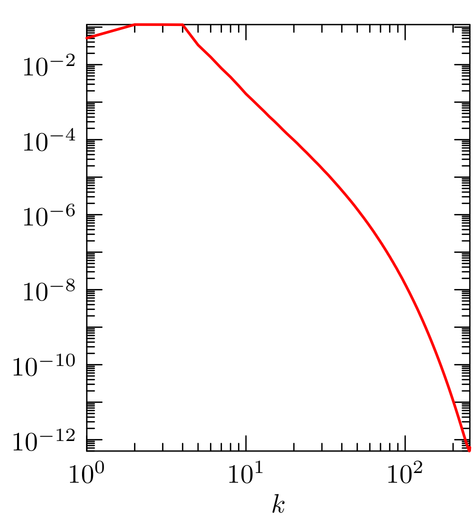

Figure 6: The steady-state energy spectrum for the simulation shown in Fig. 2.

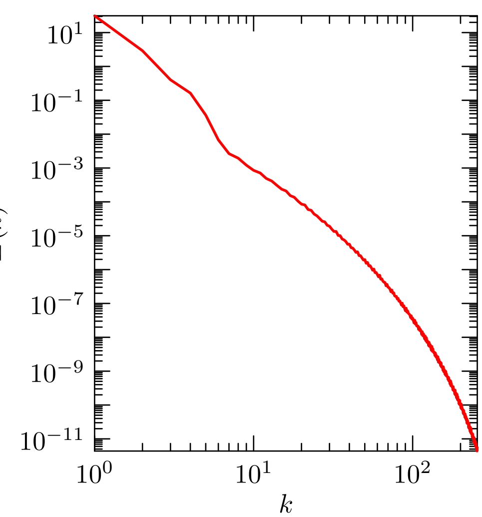

Figure 7: The quasisteady-state energy spectrum for the simulation shown in Fig. 3.

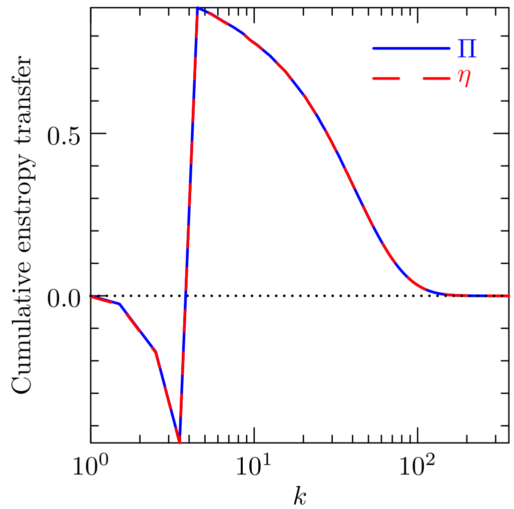

Figure 8: The enstrophy transfer for the simulation shown in Fig. 2.

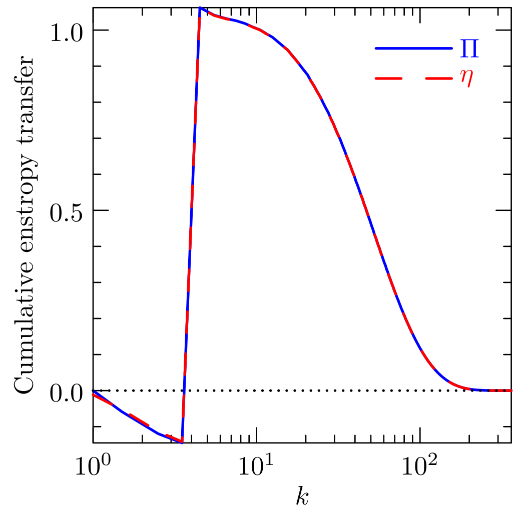

Figure 9: The enstrophy transfer for the simulation shown in Fig. 3.

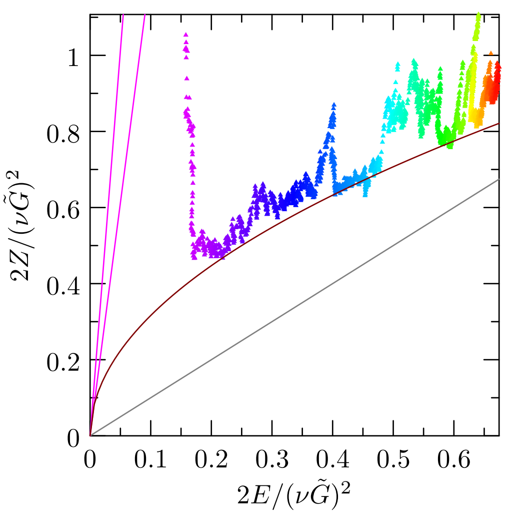

Figure 10: Enstrophy vs. energy evolution ($t > 146$) for white-noise forcing computed with 255×255 dealiased modes using $\eta = 1$, $k_f = 4$, $\delta_f = 1$, $\nu_H = 0.0005$, $\nu_L = 0$, $\alpha = 1$, and $\beta = 1$.

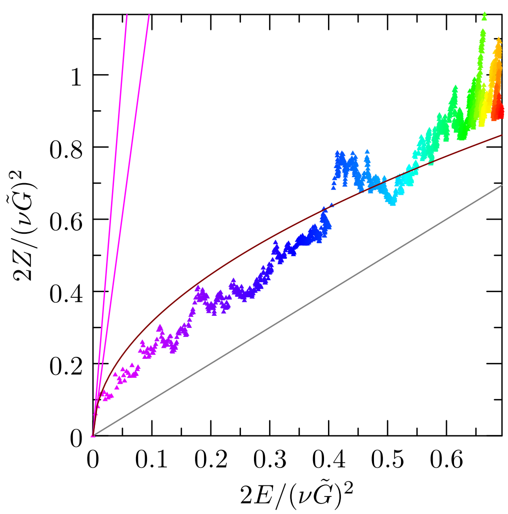

Figure 11: Enstrophy vs. energy evolution for white-noise forcing computed with 255×255 dealiased modes using $\eta = 10^{12}$, $k_f = 4$, $\delta_f = 1$, $\nu_H = 5$, $\nu_L = 0$, $\alpha = 1$, and $\beta = 1$.

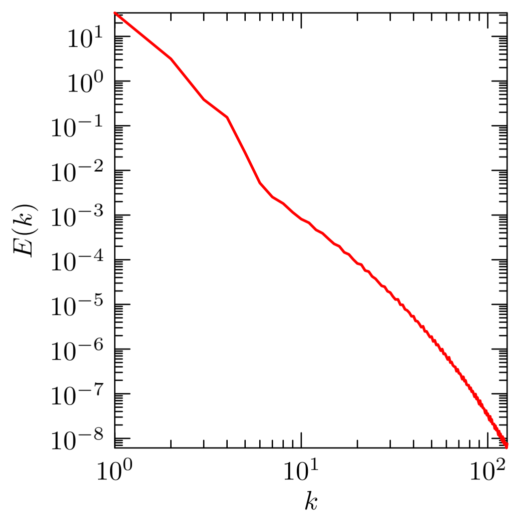

Figure 12: The quasisteady-state energy spectrum for the simulation shown in Fig. 10.

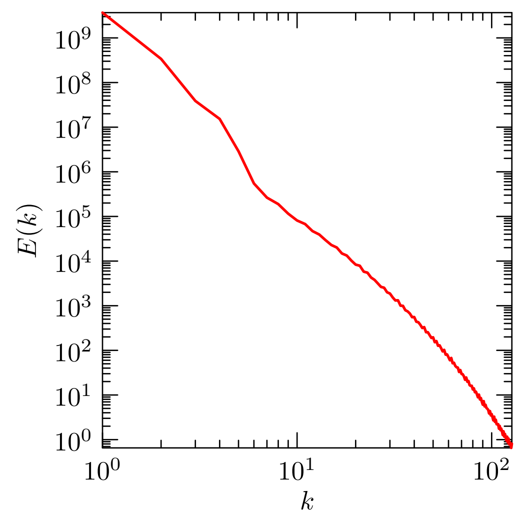

Figure 13: The quasisteady-state energy spectrum for the simulation shown in Fig. 11.

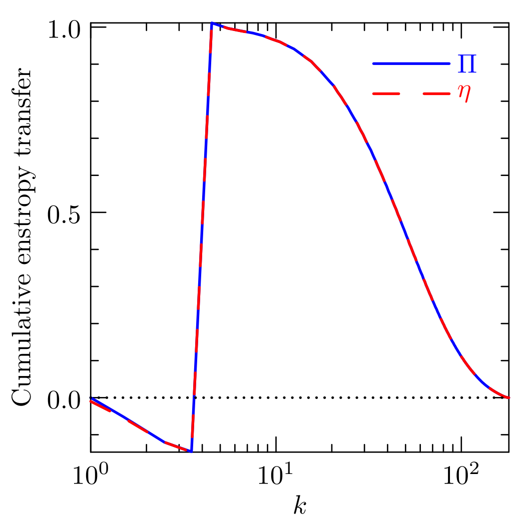

Figure 14: The enstrophy transfer for the simulation shown in Fig. 10.

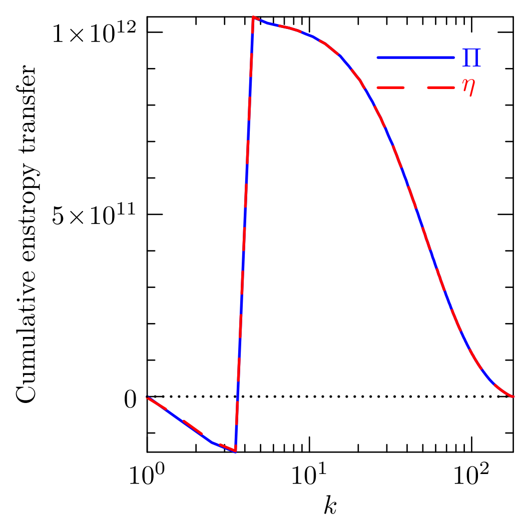

Figure 15: The enstrophy transfer for the simulation shown in Fig. 11.

To test the sensitivity of these results with respect to resolution and initial conditions, we repeated the simulation shown in Figure 2 with a larger initial condition and a lower 255×255 resolution. The corresponding energy spectrum and cumulative enstrophy transfer graphs are shown in Figures 12 and 14. The projection of the solution onto the Z–E plane is shown in Figure 10, where for illustration purposes, the evolution of the first 120 000 timesteps is omitted. Finally, Figure 11 illustrates the projection of the global attractor for $\eta = 10^{12}$ and $\nu_H = 5$, with a 255×255 resolution. Here we need to address one issue regarding the very large values of the parameters in this simulation. This issue pertains to the finite floating-point representation used on digital computers, which can result in a loss of precision. Due to the sensitivity of turbulence to the initial conditions, this issue could well cause significant discrepancies between numerical and analytical results. Nevertheless, Figure 11 demonstrates the robustness of the numerical simulation and the global attractor. Figures 13 and 15 depict the energy spectrum and transfer graphs for this simulation.

In the preceding results, we have observed excellent agreement between the theoretical predictions and high accuracy numerical simulations based on the pseudospectral method. One observes the attraction of the solutions to the global attractor, whose projection lies in the region characterized by the upper and lower bounds. We also established the robustness of the numerical simulation with respect to changes in the resolution and initial conditions. In other simulations not shown here, we verified the consistency of these numerical results with respect to changes in k_f and δ_f.

11. Discussion

The most important achievement of this work is the extension of the bounds in the Z–E plane obtained by Dascaliuc, Foias, and Jolly [2005, 2010] for 2D incompressible homogeneous isotropic turbulence, under the assumption of constant forcing, to the more realistic case of random forcing. This valuable result has a few consequences, some of which should be followed up in future work. For example:

1. The analytical bounds for random forcing provide a means to evaluate various heuristic turbulent subgrid models by characterizing the behaviour of the global attractor under these models.
2. With these tools, it should now be possible to study the relation between a specific white-noise forcing and a constant forcing by

examining their effects on the global attractor, which may lead to an explicit relation for the energy and enstrophy injection rates for constant forcing.

3. In pseudospectral simulations of high Reynolds number turbulence, refining the grid down to the Kolmogorov dissipation scale is almost impossible due to limited memory, computation time, and machine precision. For engineering applications, it is essential to somehow tackle these deficiencies. A common approach is to introduce a heuristic subgrid model, where one strives to model the damping effect of neglected small scales on larger scales. This avoids the need for a highly refined grid, significantly speeding up the simulation. Although these models are the best one can currently do as far as obtaining a crude realization of turbulence using current technology and computational resources, they are not based on a firm mathematical foundation. It is possible that analytic bounds like those discussed in this work could be used to rank subgrid models according to their mathematical reliability.
4. Analytic bounds on the projected 2D global random attractor should assist in studying artificial energy damping mechanisms designed to remove the energy that cascades upscale before it piles up and reflects off the largest scale, back towards smaller scales.

The final point about artificial large-scale damping mechanisms is an important open problem for simulations of 2D turbulence. This work raises serious questions about the impact of these damping mechanisms on the turbulent dynamics. Perhaps an awareness of the constraints on the global random attractor can guide future research in devising less invasive energy damping models.

Appendix A. Bilinear map identities

A bilinear map $\mathcal{B} : V \times V \to V$ over a vector space V is a function that is linear in each argument separately. That is, for all $\boldsymbol{u}$, $\boldsymbol{v}$, $\boldsymbol{w} \in V$, and scalars λ:

$$\begin{aligned}\mathcal{B}(\boldsymbol{u}+\boldsymbol{v},\boldsymbol{w}) = \mathcal{B}(\boldsymbol{u},\boldsymbol{w}) + \mathcal{B}(\boldsymbol{v},\boldsymbol{w}) \quad &\text{and} \quad \mathcal{B}(\lambda\boldsymbol{u},\boldsymbol{v}) = \lambda\mathcal{B}(\boldsymbol{u},\boldsymbol{v}),\\ \mathcal{B}(\boldsymbol{u},\boldsymbol{v}+\boldsymbol{w}) = \mathcal{B}(\boldsymbol{u},\boldsymbol{v}) + \mathcal{B}(\boldsymbol{u},\boldsymbol{w}) \quad &\text{and} \quad \mathcal{B}(\boldsymbol{u},\lambda\boldsymbol{v}) = \lambda\mathcal{B}(\boldsymbol{u},\boldsymbol{v}).\end{aligned}$$

The bilinear map $\mathcal{B}$ allows us to represent the Navier–Stokes equations (1) in the compact form (7).

Although the analysis in this work is limited to $[0, 2\pi]^2$, some of the identities can be extended to $\Omega_3 = [0, 2\pi]^3$, so in general let us consider a velocity vector field $\boldsymbol{u} : \Omega_3 \times \mathbb{R} \longrightarrow \mathbb{R}^3$ with $\boldsymbol{\nabla}\boldsymbol{\cdot}\boldsymbol{u} = 0$.

Appendix A.1. Antisymmetry

The bilinear map admits the identity

$$(\mathcal{B}(\boldsymbol{u}, \boldsymbol{v}), \boldsymbol{w}) = -(\mathcal{B}(\boldsymbol{u}, \boldsymbol{w}), \boldsymbol{v}), \quad \forall\ \boldsymbol{u}, \boldsymbol{v}, \boldsymbol{w} \in H(\Omega_3). \tag{A.1}$$

Having the incompressibility condition for $\boldsymbol{u}, \boldsymbol{v}$, and $\boldsymbol{w}$, we can write

$$(\mathcal{B}(\boldsymbol{u}, \boldsymbol{v}), \boldsymbol{w}) = \int_\Omega \mathcal{B}(\boldsymbol{u}, \boldsymbol{v})\boldsymbol{\cdot}\boldsymbol{w}\, d\boldsymbol{x} = \underbrace{\int_\Omega (\boldsymbol{u}\boldsymbol{\cdot}\boldsymbol{\nabla}\boldsymbol{v})\boldsymbol{\cdot}\boldsymbol{w}\, d\boldsymbol{x}}_{I} + \underbrace{\int_\Omega \boldsymbol{\nabla}p\boldsymbol{\cdot}\boldsymbol{w}\, d\boldsymbol{x}}_{J}, \tag{A.2}$$

so we have

$$\begin{aligned} I &= \int_\Omega \boldsymbol{\nabla}\boldsymbol{\cdot}(\boldsymbol{u}\boldsymbol{v}\boldsymbol{\cdot}\boldsymbol{\omega})\, d\boldsymbol{x} - \int_\Omega (\boldsymbol{\nabla}\boldsymbol{\cdot}\boldsymbol{u})\boldsymbol{v}\boldsymbol{\cdot}\boldsymbol{\omega}\, d\boldsymbol{x} - \int_\Omega (\boldsymbol{u}\boldsymbol{\cdot}\boldsymbol{\nabla}\boldsymbol{w})\boldsymbol{\cdot}\boldsymbol{v}\, d\boldsymbol{x} \\ &= \int_{\partial\Omega} (\boldsymbol{u}\boldsymbol{v}\boldsymbol{\cdot}\boldsymbol{w})\, \hat{\boldsymbol{n}}\, dS - \int_\Omega (\boldsymbol{u}\boldsymbol{\cdot}\boldsymbol{\nabla}\boldsymbol{w})\boldsymbol{\cdot}\boldsymbol{v}\, d\boldsymbol{x} = -\int_\Omega (\boldsymbol{u}\boldsymbol{\cdot}\boldsymbol{\nabla}\boldsymbol{w})\boldsymbol{\cdot}\boldsymbol{v}\, d\boldsymbol{x}, \end{aligned}$$

and similarly

$$J = \int_\Omega \boldsymbol{\nabla}\boldsymbol{\cdot}(p\boldsymbol{w})\, d\boldsymbol{x} - \int_\Omega p\boldsymbol{\nabla}\boldsymbol{\cdot}\boldsymbol{w}\, d\boldsymbol{x} = \int_{\partial\Omega} (p\boldsymbol{w})\boldsymbol{\cdot}\hat{\boldsymbol{n}}\, dS - 0 = 0,$$

where the integrals on the boundary $\partial\Omega$ vanish because of periodicity. So, (A.2) can be written as

$$(\mathcal{B}(\boldsymbol{u}, \boldsymbol{v}), \boldsymbol{w}) = I + J = -\int_\Omega (\boldsymbol{u}\boldsymbol{\cdot}\boldsymbol{\nabla}\boldsymbol{w})\boldsymbol{\cdot}\boldsymbol{v}\, d\boldsymbol{x} - \int_\Omega \boldsymbol{\nabla}p\boldsymbol{\cdot}\boldsymbol{v}\, d\boldsymbol{x} \tag{A.3}$$

$$= -\int_\Omega \mathcal{B}(\boldsymbol{u}, \boldsymbol{w})\boldsymbol{\cdot}\boldsymbol{v}\, d\boldsymbol{x} = -(\mathcal{B}(\boldsymbol{u}, \boldsymbol{w}), \boldsymbol{v}). \tag{A.4}$$

Appendix A.2. Orthogonality in two-dimensional incompressible flows

Two-dimensional incompressible flows also satisfy the orthogonality identity

$$(\mathcal{B}(\boldsymbol{u}, \boldsymbol{u}), A\boldsymbol{u}) = 0, \quad \text{where} \quad A = -\nabla^2.$$

The proof is based on standard vector calculus identities. Since $\boldsymbol{\nabla}\times\boldsymbol{\nabla}p = \boldsymbol{0}$ and, for two-dimensional flows, $\boldsymbol{\omega}\boldsymbol{\cdot}\boldsymbol{\nabla}\boldsymbol{u} = 0$, the curl of the nonlinearity $\boldsymbol{S} \doteq$

$\mathcal{B}(\boldsymbol{u},\boldsymbol{u}) = \boldsymbol{u}\cdot\boldsymbol{\nabla}\boldsymbol{u} + \boldsymbol{\nabla}p$ may be rewritten as $\boldsymbol{\nabla}\times\boldsymbol{S} = \boldsymbol{\nabla}\times(\boldsymbol{u}\cdot\boldsymbol{\nabla}\boldsymbol{u}) = \boldsymbol{u}\cdot\boldsymbol{\nabla}\boldsymbol{\omega}$. Thus

$$
\begin{aligned}
(\mathcal{B}(\boldsymbol{u},\boldsymbol{u}), A\boldsymbol{u}) &= \int_\Omega -\boldsymbol{S}\cdot\nabla^2\boldsymbol{u}\,d\boldsymbol{x} = \int_\Omega \boldsymbol{S}\cdot(\boldsymbol{\nabla}\times\boldsymbol{\omega})\,d\boldsymbol{x}\\
&= \int_\Omega \boldsymbol{\nabla}\cdot(\boldsymbol{\omega}\times\boldsymbol{S})\,d\boldsymbol{x} + \int_\Omega \boldsymbol{\omega}\cdot(\boldsymbol{\nabla}\times\boldsymbol{S})\,d\boldsymbol{x}\\
&= \int_{\partial\Omega} (\boldsymbol{\omega}\times\boldsymbol{S})\cdot\hat{\boldsymbol{n}}\,ds + \int_\Omega \boldsymbol{\omega}\cdot(\boldsymbol{u}\cdot\boldsymbol{\nabla}\boldsymbol{\omega})\,d\boldsymbol{x}\\
&= 0 + \int_\Omega \boldsymbol{u}\cdot\boldsymbol{\nabla}\left(\frac{\omega^2}{2}\right)d\boldsymbol{x} = \int_{\partial\Omega}\left(\frac{\omega^2}{2}\boldsymbol{u}\right)\cdot\hat{\boldsymbol{n}}\,ds - \int_\Omega\left(\frac{\omega^2}{2}\right)\boldsymbol{\nabla}\cdot\boldsymbol{u}\,d\boldsymbol{x} = 0,
\end{aligned}
$$

where the integrals on the boundary $\partial\Omega$ vanish because of periodicity.

Appendix A.3. Strong form of enstrophy invariance

Another useful identity for the bilinear map in two-dimensional incompressible flows is called the strong form of enstrophy invariance:

$$
(\mathcal{B}(A\boldsymbol{v},\boldsymbol{v}),\boldsymbol{u}) = (\mathcal{B}(\boldsymbol{u},\boldsymbol{v}), A\boldsymbol{v}). \tag{A.5}
$$

The proof given here is more elegant than that given by Dascaliuc et al. [7], as it elucidates the underlying fluid dynamics and vector calculus identities. We first prove the identity

$$
(\mathcal{B}(\boldsymbol{u},A\boldsymbol{v}),\boldsymbol{v}) = (\mathcal{B}(A\boldsymbol{v},\boldsymbol{u}),\boldsymbol{v}). \tag{A.6}
$$

We can write

$$
\begin{aligned}
(\mathcal{B}(\boldsymbol{u},A\boldsymbol{v}),\boldsymbol{v}) - (\mathcal{B}(A\boldsymbol{v},\boldsymbol{u}),\boldsymbol{v}) &= ([\mathcal{B}(\boldsymbol{u},A\boldsymbol{v}) - \mathcal{B}(A\boldsymbol{v},A\boldsymbol{u})],\boldsymbol{v})\\
&= \int_\Omega [\boldsymbol{u}\cdot\boldsymbol{\nabla}(A\boldsymbol{v}) - A\boldsymbol{v}\cdot\boldsymbol{\nabla}\boldsymbol{u} + \boldsymbol{\nabla}(p-p')]\cdot\boldsymbol{v}\,d\boldsymbol{x}\\
&= \int_\Omega \underbrace{(\boldsymbol{m}\cdot\boldsymbol{\nabla}\boldsymbol{n} - \boldsymbol{n}\cdot\boldsymbol{\nabla}\boldsymbol{m})\cdot\boldsymbol{v}}_{I}\,d\boldsymbol{x} + \int_\Omega \underbrace{\boldsymbol{\nabla}p_1\cdot\boldsymbol{v}}_{J}\,d\boldsymbol{x},
\end{aligned}
$$

where $\boldsymbol{m} = \boldsymbol{u}$, $\boldsymbol{n} = A\boldsymbol{v}$, and $p_1 = p - p'$. Using the vector calculus identity

$$
\boldsymbol{\nabla}\times(\boldsymbol{n}\times\boldsymbol{m}) = \boldsymbol{n}(\boldsymbol{\nabla}\cdot\boldsymbol{m}) - \boldsymbol{m}(\boldsymbol{\nabla}\cdot\boldsymbol{n}) + (\boldsymbol{m}\cdot\boldsymbol{\nabla})\boldsymbol{n} - (\boldsymbol{n}\cdot\boldsymbol{\nabla})\boldsymbol{m},
$$

I can be written as

$$
\begin{aligned}
(\boldsymbol{m}\boldsymbol{\cdot}\boldsymbol{\nabla}\boldsymbol{n} - \boldsymbol{n}\boldsymbol{\cdot}\boldsymbol{\nabla}\boldsymbol{m})\boldsymbol{\cdot}\boldsymbol{u} &= [\boldsymbol{\nabla}\times(\boldsymbol{n}\times\boldsymbol{m}) - (\boldsymbol{\nabla}\boldsymbol{\cdot}\boldsymbol{m})\boldsymbol{n} + (\boldsymbol{\nabla}\boldsymbol{\cdot}\boldsymbol{n})\boldsymbol{m}]\boldsymbol{\cdot}\boldsymbol{v} \\
&= [\boldsymbol{\nabla}\times(\boldsymbol{u}\times A\boldsymbol{v}) - (\boldsymbol{\nabla}\boldsymbol{\cdot}A\boldsymbol{v})\boldsymbol{u} + (\boldsymbol{\nabla}\boldsymbol{\cdot}\boldsymbol{u})A\boldsymbol{v}]\boldsymbol{\cdot}\boldsymbol{v} \\
&= (\boldsymbol{\nabla}\times(\boldsymbol{u}\times A\boldsymbol{v}))\boldsymbol{\cdot}\boldsymbol{v} + 0 + 0 = (\boldsymbol{\nabla}\times(\boldsymbol{u}\times A\boldsymbol{v}))\boldsymbol{\cdot}\boldsymbol{v},
\end{aligned}
$$

and J becomes

$$
\int_\Omega \boldsymbol{\nabla} p_1\boldsymbol{\cdot}\boldsymbol{u}\,d\boldsymbol{x} \overset{\boldsymbol{\nabla}\cdot\boldsymbol{u}=0}{=} \int_\Omega \boldsymbol{\nabla}\boldsymbol{\cdot}(p_1\boldsymbol{u})\,d\boldsymbol{x} = \int_{\partial\Omega} p_1\boldsymbol{u}\boldsymbol{\cdot}\hat{\boldsymbol{n}}\,ds = 0,
$$

where the last integral vanishes because of periodic boundary conditions. So we would have

$$
\begin{aligned}
((\mathcal{B}(\boldsymbol{u}, A\boldsymbol{v}) - \mathcal{B}(A\boldsymbol{v}, \boldsymbol{u})), \boldsymbol{v}) &= \int_\Omega \boldsymbol{v}\boldsymbol{\cdot}\boldsymbol{\nabla}\times(\underbrace{\boldsymbol{u}\times A\boldsymbol{v}}_{\boldsymbol{S}})\,d\boldsymbol{x} \\
&= \int_\Omega \boldsymbol{\nabla}\boldsymbol{\cdot}(\boldsymbol{S}\times\boldsymbol{v})\,d\boldsymbol{x} + \int_\Omega \boldsymbol{S}\boldsymbol{\cdot}\boldsymbol{\nabla}\times\boldsymbol{v}\,d\boldsymbol{x} \\
&= \int_{\partial\Omega} (\boldsymbol{S}\times\boldsymbol{v})\boldsymbol{\cdot}\hat{\boldsymbol{n}}\,ds + \int_\Omega \boldsymbol{\omega}\boldsymbol{\cdot}\boldsymbol{S}\,d\boldsymbol{x} = 0 + \int_\Omega \boldsymbol{\omega}\boldsymbol{\cdot}(\boldsymbol{u}\times A\boldsymbol{v})\,d\boldsymbol{x} \\
&= -\int_\Omega \boldsymbol{u}\boldsymbol{\cdot}(\boldsymbol{\omega}\times A\boldsymbol{u})\,d\boldsymbol{x} = -\int_\Omega \boldsymbol{u}\boldsymbol{\cdot}(\boldsymbol{\omega}\times(\boldsymbol{\nabla}\times\boldsymbol{\omega}))\,d\boldsymbol{x}.
\end{aligned}
$$

Using the fact that $\boldsymbol{\omega}\times(\boldsymbol{\nabla}\times\boldsymbol{\omega}) = \frac{1}{2}\boldsymbol{\nabla}\boldsymbol{\omega}^2 - \boldsymbol{\omega}\boldsymbol{\cdot}\boldsymbol{\nabla}\boldsymbol{\omega}$, and since in the two-dimensional case $\boldsymbol{\omega}\boldsymbol{\cdot}\boldsymbol{\nabla}\boldsymbol{\omega} = \boldsymbol{0}$, we obtain

$$
\begin{aligned}
((\mathcal{B}(\boldsymbol{u}, A\boldsymbol{v}) - \mathcal{B}(A\boldsymbol{v}, \boldsymbol{u})), \boldsymbol{v}) &= -\int_\Omega \boldsymbol{u}\boldsymbol{\cdot}(\boldsymbol{\omega}\times(\boldsymbol{\nabla}\times\boldsymbol{\omega}))\,d\boldsymbol{x} = -\int_\Omega \boldsymbol{u}\boldsymbol{\cdot}\left(\frac{1}{2}\boldsymbol{\nabla}\omega^2\right)d\boldsymbol{x} \\
&= -\int_\Omega \boldsymbol{u}\boldsymbol{\cdot}\left(\frac{1}{2}\boldsymbol{\nabla}\omega^2\right)d\boldsymbol{x} = -\int_\Omega \boldsymbol{u}\boldsymbol{\cdot}\left(\frac{1}{2}\boldsymbol{\nabla}\omega^2\right)d\boldsymbol{x} \\
&= -\int_\Omega \boldsymbol{\nabla}\boldsymbol{\cdot}\left(\frac{\boldsymbol{u}\omega^2}{2}\right)d\boldsymbol{x} = -\int_{\partial\Omega}\left(\frac{\boldsymbol{u}\omega^2}{2}\right)\boldsymbol{\cdot}\hat{\boldsymbol{n}}\,ds = 0,
\end{aligned}
$$

and so (A.6) follows. Having this identity, we can write

$$
(\mathcal{B}(A\boldsymbol{v}, \boldsymbol{v}), \boldsymbol{u}) \overset{(A.1)}{=} -(\mathcal{B}(A\boldsymbol{v}, \boldsymbol{u}), \boldsymbol{v}) \overset{(A.6)}{=} -(\mathcal{B}(\boldsymbol{u}, A\boldsymbol{v}), \boldsymbol{v}) \overset{(A.1)}{=} (\mathcal{B}(\boldsymbol{u}, \boldsymbol{v}), A\boldsymbol{v}),
$$

which proves (A.5).

Appendix A.4. General identity in two-dimensional incompressible flow

Using the above identities it is possible to show that

$$\underbrace{(\mathcal{B}(\boldsymbol{v},\boldsymbol{v}),A\boldsymbol{u})}_{I}+\underbrace{(\mathcal{B}(\boldsymbol{v},\boldsymbol{u}),A\boldsymbol{v})}_{II}+\underbrace{(\mathcal{B}(\boldsymbol{u},\boldsymbol{v}),A\boldsymbol{v})}_{III}=0. \tag{A.7}$$

As in the previous section there is another proof given by Foias et al. [9], and although their proof is much more concise, it is completely based on the functional analysis properties of the bilinear map. In contrast, the following proof is based on vector calculus identities, which are more insightful, especially for physically oriented readers. We begin with the term I:

$$(\mathcal{B}(\boldsymbol{v},\boldsymbol{v}),A\boldsymbol{u})=\int_\Omega(\boldsymbol{v}\boldsymbol{\cdot}\boldsymbol{\nabla}\boldsymbol{v}+\boldsymbol{\nabla}p)\boldsymbol{\cdot}(-\nabla^2\boldsymbol{u})\,d\boldsymbol{x}=\int_\Omega(\boldsymbol{v}\boldsymbol{\cdot}\boldsymbol{\nabla}\boldsymbol{v})\boldsymbol{\cdot}(-\nabla^2\boldsymbol{u})\,d\boldsymbol{x}.$$

Let $\boldsymbol{\omega}=\boldsymbol{\nabla}\times\boldsymbol{u}$, so that $-\nabla^2\boldsymbol{u}=\boldsymbol{\nabla}\times\boldsymbol{\omega}$, and consequently we obtain

$$\begin{aligned}
(\mathcal{B}(\boldsymbol{v},\boldsymbol{v}),A\boldsymbol{u}) &= \int_\Omega(\boldsymbol{v}\boldsymbol{\cdot}\boldsymbol{\nabla}\boldsymbol{v})\boldsymbol{\cdot}\boldsymbol{\nabla}\times\boldsymbol{\omega}\,d\boldsymbol{x}\\
&= \int_\Omega\boldsymbol{\nabla}\boldsymbol{\cdot}(\boldsymbol{\omega}\times(\boldsymbol{v}\boldsymbol{\cdot}\boldsymbol{\nabla}\boldsymbol{v}))\,d\boldsymbol{x}+\int_\Omega\boldsymbol{\omega}\boldsymbol{\cdot}\boldsymbol{\nabla}\times(\boldsymbol{v}\boldsymbol{\cdot}\boldsymbol{\nabla}\boldsymbol{v})\,d\boldsymbol{x}\\
&= \int_{\partial\Omega}\boldsymbol{\omega}\times(\boldsymbol{v}\boldsymbol{\cdot}\boldsymbol{\nabla}\boldsymbol{v})\boldsymbol{\cdot}\hat{\boldsymbol{n}}\,ds+\int_\Omega\boldsymbol{\omega}\boldsymbol{\cdot}\boldsymbol{\nabla}\times(\boldsymbol{v}\boldsymbol{\cdot}\boldsymbol{\nabla}\boldsymbol{v})\,d\boldsymbol{x}\\
&= 0+\int_\Omega\boldsymbol{\omega}\boldsymbol{\cdot}\underbrace{\boldsymbol{\nabla}\times(\boldsymbol{v}\boldsymbol{\cdot}\boldsymbol{\nabla}\boldsymbol{v})}_{\boldsymbol{S}}\,d\boldsymbol{x}=\int_\Omega\boldsymbol{S}\boldsymbol{\cdot}(\boldsymbol{\nabla}\times\boldsymbol{u})\,d\boldsymbol{x}\\
&= \int_\Omega\boldsymbol{\nabla}\boldsymbol{\cdot}(\boldsymbol{u}\times\boldsymbol{S})\,d\boldsymbol{x}+\int_\Omega\boldsymbol{u}\boldsymbol{\cdot}\boldsymbol{\nabla}\times\boldsymbol{S}\,d\boldsymbol{x}\\
&= \int_{\partial\Omega}(\boldsymbol{u}\times\boldsymbol{S})\boldsymbol{\cdot}\hat{\boldsymbol{n}}\,ds+\int_\Omega\boldsymbol{u}\boldsymbol{\cdot}\boldsymbol{\nabla}\times\boldsymbol{S}\,d\boldsymbol{x}\\
&= 0+\int_\Omega\boldsymbol{u}\boldsymbol{\cdot}\boldsymbol{\nabla}\times\boldsymbol{S}\,d\boldsymbol{x}=\int_\Omega\boldsymbol{u}\boldsymbol{\cdot}\boldsymbol{\nabla}\times\boldsymbol{S}\,d\boldsymbol{x}.
\end{aligned}$$

On the other hand we have

$$\boldsymbol{S}=\boldsymbol{\nabla}\times(\boldsymbol{v}\boldsymbol{\cdot}\boldsymbol{\nabla}\boldsymbol{v})=\boldsymbol{\nabla}\times\left(\boldsymbol{\nabla}\frac{v^2}{2}\right)-\boldsymbol{\nabla}\times(\boldsymbol{v}\times(\boldsymbol{\nabla}\times\boldsymbol{v}))=-\boldsymbol{\nabla}\times(\boldsymbol{v}\times(\underbrace{\boldsymbol{\nabla}\times\boldsymbol{v}}_{\boldsymbol{w}})).$$

But

$$\boldsymbol{S}=-\boldsymbol{\nabla}\times(\boldsymbol{v}\times\boldsymbol{w})=-[\boldsymbol{v}(\boldsymbol{\nabla}\boldsymbol{\cdot}\boldsymbol{w})-\boldsymbol{w}(\boldsymbol{\nabla}\boldsymbol{\cdot}\boldsymbol{v})+(\boldsymbol{w}\boldsymbol{\cdot}\boldsymbol{\nabla})\boldsymbol{v}-(\boldsymbol{v}\boldsymbol{\cdot}\boldsymbol{\nabla})\boldsymbol{w}]=(\boldsymbol{v}\boldsymbol{\cdot}\boldsymbol{\nabla})\boldsymbol{w}.$$

On considering the fact that $(\boldsymbol{w}\cdot\boldsymbol{\nabla})\boldsymbol{v}=0$, we can write

$$\begin{aligned}\boldsymbol{S}=(\boldsymbol{v}\cdot\boldsymbol{\nabla})\boldsymbol{w}&=\boldsymbol{\nabla}(\boldsymbol{v}\cdot\boldsymbol{w})-\boldsymbol{w}\cdot\boldsymbol{\nabla}\boldsymbol{v}-\boldsymbol{v}\times(\boldsymbol{\nabla}\times\boldsymbol{w})-\boldsymbol{w}\times(\boldsymbol{\nabla}\times\boldsymbol{v})\\ &=0-0-\boldsymbol{v}\times(\boldsymbol{\nabla}\times\boldsymbol{w})-0\\ &=-\boldsymbol{v}\times(\boldsymbol{\nabla}\times\boldsymbol{w})=-\boldsymbol{v}\times(\boldsymbol{\nabla}\times(\boldsymbol{\nabla}\times\boldsymbol{v}))=-\boldsymbol{v}\times(\boldsymbol{\nabla}(\boldsymbol{\nabla}\cdot\boldsymbol{v})-\nabla^2\boldsymbol{v})\\ &=\boldsymbol{v}\times\nabla^2\boldsymbol{v}.\end{aligned}$$

Thus

$$\begin{aligned}\boldsymbol{\nabla}\times\boldsymbol{S}&=\boldsymbol{\nabla}\times(\boldsymbol{v}\times\nabla^2\boldsymbol{v})\\ &=\boldsymbol{v}(\boldsymbol{\nabla}\cdot\nabla^2\boldsymbol{v})-\nabla^2\boldsymbol{v}(\boldsymbol{\nabla}\cdot\boldsymbol{v})+((\nabla^2\boldsymbol{v})\cdot\boldsymbol{\nabla})\boldsymbol{v}-(\boldsymbol{v}\cdot\boldsymbol{\nabla})\nabla^2\boldsymbol{v}\\ &=0-0+(\nabla^2\boldsymbol{v}\cdot\boldsymbol{\nabla})\boldsymbol{v}-(\boldsymbol{v}\cdot\boldsymbol{\nabla})\nabla^2\boldsymbol{v}=(\nabla^2\boldsymbol{v}\cdot\boldsymbol{\nabla})\boldsymbol{v}-(\boldsymbol{v}\cdot\boldsymbol{\nabla})\nabla^2\boldsymbol{v}.\end{aligned}$$

So in the end we obtain

$$(\mathcal{B}(\boldsymbol{v},\boldsymbol{v}),A\boldsymbol{u})=\int_\Omega(\boldsymbol{\nabla}\times\boldsymbol{S})\cdot\boldsymbol{u}\,d\boldsymbol{x}=\int_\Omega(\nabla^2\boldsymbol{v}\cdot\boldsymbol{\nabla}\boldsymbol{v})\cdot\boldsymbol{u}\,d\boldsymbol{x}-\int_\Omega(\boldsymbol{v}\cdot\boldsymbol{\nabla}\nabla^2\boldsymbol{v})\cdot\boldsymbol{u}\,d\boldsymbol{x}.$$

On noting that we can add or subtract terms of the form $\int_\Omega\boldsymbol{u}\cdot\boldsymbol{\nabla}p\,d\boldsymbol{x}=0$, we can write

$$\begin{aligned}(\mathcal{B}(\boldsymbol{v},\boldsymbol{v}),A\boldsymbol{u})&=\int_\Omega((\nabla^2\boldsymbol{v}\cdot\boldsymbol{\nabla})\boldsymbol{v})\cdot\boldsymbol{u}\,d\boldsymbol{x}-\int_\Omega((\boldsymbol{v}\cdot\boldsymbol{\nabla})\nabla^2\boldsymbol{v})\cdot\boldsymbol{u}\,d\boldsymbol{x}\\ &=-(\mathcal{B}(A\boldsymbol{v},\boldsymbol{v}),\boldsymbol{u})+(\mathcal{B}(\boldsymbol{v},A\boldsymbol{v}),\boldsymbol{u}).\end{aligned}$$

Up to this point we have found a valuable representation of the term I in (A.7):

$$(\mathcal{B}(\boldsymbol{v},\boldsymbol{v}),A\boldsymbol{u})=\underbrace{(\mathcal{B}(\boldsymbol{v},A\boldsymbol{v}),\boldsymbol{u})}_{J}-\underbrace{(\mathcal{B}(A\boldsymbol{v},\boldsymbol{v}),\boldsymbol{u})}_{K}. \tag{A.8}$$

Applying identities (A.1) and (A.5) respectively to the terms J and K, we obtain

$$(\mathcal{B}(\boldsymbol{v},\boldsymbol{v}),A\boldsymbol{u})=-(\mathcal{B}(\boldsymbol{v},\boldsymbol{u}),A\boldsymbol{v})-(\mathcal{B}(\boldsymbol{u},\boldsymbol{v}),A\boldsymbol{v}),$$

which is exactly (A.7).

Appendix A.5. Estimates for the bilinear term involving powers of the Stokes operator

A term that has great impact on our analysis of the Navier–Stokes equations is $(\mathcal{B}(\boldsymbol{v},\boldsymbol{v}),A^2\boldsymbol{v})$. Having a good estimate for this term is vital in our work, but unfortunately no simpler representation is known for this term, only a useful upper bound. Using the equivalent form of the general 2D identity, (A.8), one obtains

$$\big(\mathcal{B}(\boldsymbol{v},\boldsymbol{v}),A^2\boldsymbol{v}\big)=(\mathcal{B}(\boldsymbol{v},\boldsymbol{v}),AA\boldsymbol{v})\overset{\boldsymbol{u}\doteq A\boldsymbol{v}}{=}(\mathcal{B}(\boldsymbol{v},\boldsymbol{v}),A\boldsymbol{u}) \tag{A.9}$$

$$\overset{(A.8)}{=}(\mathcal{B}(\boldsymbol{v},A\boldsymbol{v}),\boldsymbol{u})-(\mathcal{B}(A\boldsymbol{v},\boldsymbol{v}),\boldsymbol{u}) \tag{A.10}$$

$$=(\mathcal{B}(\boldsymbol{v},A\boldsymbol{v}),A\boldsymbol{v})-(\mathcal{B}(A\boldsymbol{v},\boldsymbol{v}),A\boldsymbol{v}) \tag{A.11}$$

$$=-(\mathcal{B}(A\boldsymbol{v},\boldsymbol{v}),A\boldsymbol{v})=(\mathcal{B}(A\boldsymbol{v},A\boldsymbol{v}),\boldsymbol{v}). \tag{A.12}$$

The above result is the best exact estimate that we could obtain using the general identity (A.7) and the other identities proven so far. As this term appears in our functional estimates, it is necessary to come up with an upper bound. In order to obtain this estimate we will eventually require the Ladyzhenskaya inequality that we introduced before:

$$\big(\mathcal{B}(\boldsymbol{u},\boldsymbol{u}),A^2\boldsymbol{u}\big)=(\mathcal{B}(A\boldsymbol{u},A\boldsymbol{u}),\boldsymbol{u})\overset{\boldsymbol{v}\doteq A\boldsymbol{u}}{=}(\mathcal{B}(\boldsymbol{v},\boldsymbol{v}),\boldsymbol{u}).$$

As we have shown earlier, the $\boldsymbol{\nabla}p$ term will vanish due to incompressibility, so

$$\begin{aligned}\big(\mathcal{B}(\boldsymbol{u},\boldsymbol{u}),A^2\boldsymbol{u}\big)&=(\mathcal{B}(\boldsymbol{v},\boldsymbol{v}),\boldsymbol{u})\\&=\int_\Omega(\boldsymbol{v}\boldsymbol{\cdot}\boldsymbol{\nabla}\boldsymbol{v})\boldsymbol{\cdot}\boldsymbol{u}\,d\boldsymbol{x}=\int_\Omega\left[\frac{1}{2}\boldsymbol{\nabla}v^2-\boldsymbol{v}\times(\boldsymbol{\nabla}\times\boldsymbol{v})\right]\boldsymbol{\cdot}\boldsymbol{u}\,d\boldsymbol{x}\\&=\int_\Omega\left(\frac{1}{2}\boldsymbol{\nabla}v^2\right)\boldsymbol{\cdot}\boldsymbol{u}\,d\boldsymbol{x}-\int_\Omega[\boldsymbol{v}\times(\boldsymbol{\nabla}\times\boldsymbol{v})]\boldsymbol{\cdot}\boldsymbol{u}\,d\boldsymbol{x}\\&=0-\int_\Omega(\boldsymbol{v}\times\boldsymbol{\omega})\boldsymbol{\cdot}\boldsymbol{u}\,d\boldsymbol{x}=\int_\Omega(\boldsymbol{\omega}\times\boldsymbol{v})\boldsymbol{\cdot}\boldsymbol{u}\,d\boldsymbol{x}.\end{aligned}$$

Using the triple product identities, we can write

$$
\begin{aligned}
\big(\mathcal{B}(\boldsymbol{u},\boldsymbol{u}), A^2\boldsymbol{u}\big) &= \int_\Omega \boldsymbol{u}\boldsymbol{\cdot}\boldsymbol{\omega}\times\boldsymbol{v}\, d\boldsymbol{x} = \int_\Omega \boldsymbol{\omega}\boldsymbol{\cdot}\boldsymbol{v}\times\boldsymbol{u}\, d\boldsymbol{x} \\
&\overset{\text{Cauchy-Schwarz}}{\leq} \left(\int_\Omega |\boldsymbol{v}\times\boldsymbol{u}|^2\, d\boldsymbol{x}\right)^{1/2} \left(\int_\Omega |\boldsymbol{\omega}|^2\, d\boldsymbol{x}\right)^{1/2} \\
&\leq \left(\int_\Omega v^2u^2\, d\boldsymbol{x}\right)^{1/2} \left(\int_\Omega \omega^2 d\boldsymbol{x}\right)^{1/2} \\
&= \left(\int_\Omega A^2u^4\, d\boldsymbol{x}\right)^{1/2} \left(\int_\Omega \omega^2 d\boldsymbol{x}\right)^{1/2} \\
&= \left(\int_\Omega (A^{1/2}u)^4\, d\boldsymbol{x}\right)^{1/2} \left(\int_\Omega \omega^2 d\boldsymbol{x}\right)^{1/2}.
\end{aligned}
$$

On the other hand we have

$$
\begin{aligned}
\int_\Omega \omega^2 d\boldsymbol{x} &= \int_\Omega |\boldsymbol{\nabla}\times\boldsymbol{v}|^2 d\boldsymbol{x} = \int_\Omega A^2|\boldsymbol{\nabla}\times\boldsymbol{u}|^2 d\boldsymbol{x} \\
&= \int_\Omega A^2\boldsymbol{\nabla}\boldsymbol{\cdot}(\boldsymbol{u}\times\boldsymbol{\omega})\, d\boldsymbol{x} + \int_\Omega A^2(\boldsymbol{u}\boldsymbol{\cdot}(-\nabla^2\boldsymbol{u}))\, d\boldsymbol{x} \\
&= 0 + \int_\Omega A^2(\boldsymbol{u}\boldsymbol{\cdot}A\boldsymbol{u}) d\boldsymbol{x} = \int_\Omega A^2(A^{1/2}\boldsymbol{u}\boldsymbol{\cdot}A^{1/2}\boldsymbol{u}) d\boldsymbol{x} \\
&= \int_\Omega A^3u^2 d\boldsymbol{x} = \left|A^{3/2}\boldsymbol{u}\right|^2.
\end{aligned}
$$

Thus we will obtain

$$
\begin{aligned}
\big(\mathcal{B}(\boldsymbol{u},\boldsymbol{u}), A^2\boldsymbol{u}\big) &\leq \left(\int_\Omega (A^{1/2}u)^4\, d\boldsymbol{x}\right)^{1/2} \left|A^{3/2}\boldsymbol{u}\right| \\
&\overset{\text{Ladyzhenskaya}}{\leq} c_L||\boldsymbol{u}||\,|A\boldsymbol{u}|\,\left|A^{3/2}\boldsymbol{u}\right|.
\end{aligned}
$$

Appendix B. Energy injection due to white-noise forcing

In this appendix we consider the Navier–Stokes equations driven by a white-noise force in preparation for the numerical simulation results that use this type of random forcing. The Novikov theorem plays an essential role in prescribing the amplitude of the white-noise forcing:

Theorem 4 (Novikov 1964)**.** *Let $\boldsymbol{v} = (v_1, v_2, \cdots, v_n)$ be a vector-valued centered Gaussian random variable and let f be a differentiable function of n variables, then assuming all averages exists,*

$$\langle v_i f(v_1, v_2, \cdots, v_n) \rangle = \Gamma_{ij} \left\langle \frac{\partial f}{\partial v_j} \right\rangle,$$

where $\Gamma_{ij} = \langle v_i v_j \rangle$.

Proof. *See Frisch [13].* ■

We begin with the momentum equation

$$\frac{\partial \boldsymbol{u}}{\partial t} + \nu A \boldsymbol{u} + \mathcal{B}(\boldsymbol{u}, \boldsymbol{u}) = \boldsymbol{f},$$

recalling that $\boldsymbol{f}$ is a general random force. A particular random force of interest to us is an isotropic Gaussian white-noise solenoidal force with the following Fourier transform $\boldsymbol{f_k}$:

$$\boldsymbol{f_k}(t) = F_{\boldsymbol{k}} \left(\mathbf{1} - \frac{\boldsymbol{kk}}{k^2} \right) \boldsymbol{\cdot} \boldsymbol{\xi_k}(t), \quad \boldsymbol{k} \boldsymbol{\cdot} \boldsymbol{f_k} = 0,$$

where $F_{\boldsymbol{k}}$ is a real number and $\boldsymbol{\xi_k}(t)$ is a unit central real Gaussian random 2D vector that satisfies $\langle \boldsymbol{\xi_k}(t) \boldsymbol{\xi_{k'}}(t') \rangle = \delta_{\boldsymbol{kk'}} \mathbf{1} \delta(t - t')$. This implies

$$\begin{aligned} \langle \boldsymbol{f_k}(t) \boldsymbol{\cdot} \boldsymbol{f_{k'}}(t') \rangle &= F_{\boldsymbol{k}} F_{\boldsymbol{k'}} \left(\delta_{ij} - \frac{k_i k_j}{k^2} \right) \langle \xi_{\boldsymbol{k}j}(t) \xi_{\boldsymbol{k'}j'}(t') \rangle \left(\delta_{j'i} - \frac{k'_{j'} k'_i}{k'^2} \right) \\ &= F_{\boldsymbol{k}}^2 \delta_{\boldsymbol{k},\boldsymbol{k'}} \delta(t - t') \left(\mathbf{1} - \frac{\boldsymbol{kk}}{k^2} \right) \boldsymbol{:} \left(\mathbf{1} - \frac{\boldsymbol{kk}}{k^2} \right) = F_{\boldsymbol{k}}^2 \delta_{\boldsymbol{k},\boldsymbol{k'}} \delta(t - t'). \end{aligned}$$

Integration of the energy equation leads to

$$\boldsymbol{u_k}(t) = \boldsymbol{u_{k'}}(t') + \int_{t'}^{t} A_{\boldsymbol{k}}[\boldsymbol{u}(\tau)] d\tau + \int_{t'}^{t} \boldsymbol{f_k}(\tau) d\tau,$$

where $A_{\boldsymbol{k}}$ is an unknown functional of the velocity field such that $\dfrac{\delta A_{\boldsymbol{k}}[\boldsymbol{u}(\tau)]}{\delta \boldsymbol{f_{k'}}(t')}$ is bounded. The nonlinear Green's function is then

$$\frac{\delta \boldsymbol{u_k}(t)}{\delta \boldsymbol{f_{k'}}(t')} = \int_{t'}^{t} \frac{\delta A_{\boldsymbol{k}}[\boldsymbol{u}(\tau)]}{\delta \boldsymbol{f_{k'}}(t')} d\tau + \int_{t'}^{t} \delta_{\boldsymbol{kk'}} \mathbf{1} \delta(\tau - t') d\tau = \int_{t'}^{t} \frac{\delta A_{\boldsymbol{k}}[\boldsymbol{u}(\tau)]}{\delta \boldsymbol{f_{k'}}(t')} d\tau + \delta_{\boldsymbol{kk'}} \mathbf{1} H(t - t'),$$

where H is the Heaviside unit step function. The Novikov theorem then allows the energy injection rate ϵ for white-noise forcing to be prescribed:

$$\begin{aligned}\epsilon = (\boldsymbol{f}(\boldsymbol{x},t), \boldsymbol{u}(\boldsymbol{x},t)) &= \int_\Omega \langle \boldsymbol{f}(\boldsymbol{x},t)\boldsymbol{\cdot}\boldsymbol{u}(\boldsymbol{x},t)\rangle\, d\boldsymbol{x} = \operatorname{Re}\sum_{\boldsymbol{k}} \langle \boldsymbol{f}_{\boldsymbol{k}}(t)\boldsymbol{\cdot}\overline{\boldsymbol{u}}_{\boldsymbol{k}}(t)\rangle \\ &= \operatorname{Re}\sum_{\boldsymbol{k},\boldsymbol{k}'} \int \left\langle \boldsymbol{f}_{\boldsymbol{k}}(t)\overline{\boldsymbol{f}}_{\boldsymbol{k}'}(t')\right\rangle \boldsymbol{:} \left\langle \frac{\delta\overline{\boldsymbol{u}}_{\boldsymbol{k}}(t)}{\delta\overline{\boldsymbol{f}}_{\boldsymbol{k}'}(t')}\right\rangle dt' \\ &= \sum_{\boldsymbol{k}} F_{\boldsymbol{k}}^2 \left(\boldsymbol{1} - \frac{\boldsymbol{k}\boldsymbol{k}}{k^2}\right) \boldsymbol{:} \left(\boldsymbol{1} - \frac{\boldsymbol{k}\boldsymbol{k}}{k^2}\right) H(0) = \frac{1}{2}\sum_{\boldsymbol{k}} F_{\boldsymbol{k}}^2\end{aligned}$$

since $H(0) = \dfrac{1}{2}$. Likewise, the enstrophy injection rate is $\eta = \dfrac{1}{2}\sum_{\boldsymbol{k}} k^2 F_{\boldsymbol{k}}^2$.

Appendix C. Basdevant formulation

Appendix C.1. 3D case

The incompressibility condition (2) can be used to rewrite the momentum equation (1) in terms of the symmetric tensor $D_{ij} = u_i u_j$:

$$\frac{\partial u_i}{\partial t} + \frac{\partial D_{ij}}{\partial x_j} = -\frac{\partial p}{\partial x_i} + \nu \frac{\partial^2 u_i}{\partial x_j^2} + F_i. \tag{C.1}$$

A naive implementation of the pseudospectral method for this equation requires three backward FFTs to compute the velocity components from their spectral representations and six forward FFTs of the independent components of D_{ij}, for a total of nine FFTs per integration stage. However Basdevant [1] showed that this number can be reduced to eight, by subtracting the divergence of the symmetric matrix $S_{ij} = \delta_{ij} \operatorname{tr} D/3$ from both sides of (C.1):

$$\frac{\partial u_i}{\partial t} + \frac{\partial (D_{ij} - S_{ij})}{\partial x_j} = -\frac{\partial (p\delta_{ij} + S_{ij})}{\partial x_j} + \nu \frac{\partial^2 u_i}{\partial x_j^2} + F_i. \tag{C.2}$$

Since the symmetric matrix $D_{ij} - S_{ij}$ is traceless, it has just five independent components. Together with the three backward FFTs required for the velocity components u_i, we see that only eight FFTs are required per integration stage. The effective pressure $p\delta_{ij} + S_{ij}$ is solved as usual from the inverse Laplacian of the force minus the nonlinearity.

Appendix C.2. 2D case

On taking the curl of (1), the vorticity $\boldsymbol{\omega}$ is seen to evolve according to

$$\frac{\partial \boldsymbol{\omega}}{\partial t} + (\boldsymbol{u}\boldsymbol{\cdot}\boldsymbol{\nabla})\boldsymbol{\omega} = (\boldsymbol{\omega}\boldsymbol{\cdot}\boldsymbol{\nabla})\boldsymbol{u} + \nu\nabla^2\boldsymbol{\omega} + \boldsymbol{\nabla}\times\boldsymbol{F},$$

where in two dimensions the vortex stretching term $(\boldsymbol{\omega}\boldsymbol{\cdot}\boldsymbol{\nabla})\boldsymbol{u}$ vanishes and $\boldsymbol{\omega}$ is normal to the plane of motion.

For C^2 velocity fields, the curl of the nonlinear term can be written in terms of $\mathsf{T}D_{ij} \doteq D_{ij} - S_{ij}$:

$$\frac{\partial}{\partial x_1}\frac{\partial}{\partial x_j}\,\mathsf{T}\,D_{2j} - \frac{\partial}{\partial x_2}\frac{\partial}{\partial x_j}\,\mathsf{T}\,D_{1j} = \left(\frac{\partial^2}{\partial x_1^2} - \frac{\partial^2}{\partial x_2^2}\right)D_{12} + \frac{\partial}{\partial x_1}\frac{\partial}{\partial x_2}(D_{22} - D_{11}),$$

on recalling that S is diagonal and $S_{11} = S_{22}$. The scalar vorticity ω then evolves according to

$$\frac{\partial \omega}{\partial t} + \left(\frac{\partial^2}{\partial x_1^2} - \frac{\partial^2}{\partial x_2^2}\right)(u_1u_2) + \frac{\partial^2}{\partial x_1 \partial x_2}\left(u_2^2 - u_1^2\right) = \nu\nabla^2\omega + \frac{\partial F_2}{\partial x_1} - \frac{\partial F_1}{\partial x_2}.$$

Two backward FFTs are required to compute u_1 and u_2 in physical space, from which the quantities u_1u_2 and $u_2^2 - u_1^2$ can be calculated and then transformed to Fourier space with two additional forward FFTs. The advective term in 2D can thus be calculated with just four FFTs.

Acknowledgments

The authors would like to thank Profs. Edriss Titi, Michael Jolly, Xinwei Yu, Brendan Pass, and Morris Flynn for insightful discussions related to this work. Financial support for this work was provided by Discovery Grant RES0020458 from the Natural Sciences and Engineering Research Council of Canada.

References

[1] Basdevant, C., 1983. Technical improvements for direct numerical simulation of homogeneous three-dimensional turbulence. Journal of Computational Physics 50 (2), 209–214.

[2] Batchelor, G. K., 1969. Computation of the energy spectrum in homogeneous two-dimensional turbulence. Phys. Fluids 12 II, 233–239.

[3] Bowman, J. C., Roberts, M., 2011. Efficient dealiased convolutions without padding. SIAM J. Sci. Comput. 33 (1), 386–406.

[4] Bowman, J. C., Roberts, M., May 6, 2010. `FFTW++`: A fast Fourier transform C^{++} header class for the `FFTW3` library. http://fftwpp.sourceforge.net.

[5] Crauel, H., Debussche, A., Flandoli, F., 1997. Random attractors. Journal of Dynamics and Differential Equations 9 (2), 307–341.

[6] Dascaliuc, R., Foias, C., Jolly, M., 2007. Universal bounds on the attractor of the navier-stokes equation in the energy, enstrophy plane. Journal of mathematical physics 48 (6), 065201.

[7] Dascaliuc, R., Foias, C., Jolly, M., 2010. Estimates on enstrophy, palinstrophy, and invariant measures for 2-D turbulence. Journal of Differential Equations 248 (4), 792–819.

[8] Dascaliuc, R., Jolly, M., Foias, C., 2005. Relations between energy and enstrophy on the global attractor of the 2-D Navier–Stokes equations. Journal of Dynamics and Differential Equations 17 (4), 643–736.

[9] Foias, C., Jolly, M., Manley, O., Rosa, R., 2002. Statistical estimates for the Navier–Stokes equations and the Kraichnan theory of 2-d fully developed turbulence. Journal of Statistical Physics 108 (3-4), 591–645.

[10] Foias, C., Jolly, M. S., Yang, M., Jun 2013. On single mode forcing of the 2d-nse. Journal of Dynamics and Differential Equations 25 (2), 393–433.

[11] Foias, C., Prodi, G., 1967. Sur le comportement global des solutions non-stationnaires des équations de Navier–Stokes en dimension 2. Rendiconti del Seminario Matematico della Università di Padova 39, 1–34.

[12] Foias, C., Temam, R., 1979. Some analytic and geometric properties of the solutions of the evolution navier-stokes equations. Journal de mathematiques pures et appliquees 58 (3), 339–368.

[13] Frisch, U., 1995. Turbulence: The Legacy of A.N.Kolmogorov. Cambdridge University Press.

[14] Kraichnan, R. H., 1959. The structure of isotropic turbulence at very high Reynolds numbers. J. Fluid Mech. 5, 497–543.

[15] Kraichnan, R. H., July 1967. Inertial ranges in two-dimensional turbulence. Phys. Fluids 10 (7), 1417–1423.

[16] Ladyzhenskaya, O., 1975. A dynamical system generated by the navier-stokes equations. Journal of Soviet Mathematics 3 (4), 458–479.

[17] Leith, C. E., March 1971. Atmospheric predictability and two-dimensional turbulence. J. Atmos. Sci. 28 (2), 145–161.

[18] Roberts, M., Bowman, J. C., 2017. Multithreaded implicitly dealiased convolutions. Submitted to Journal of Computational Physics.

[19] Temam, R., 1995. Navier–Stokes equations and nonlinear functional analysis. SIAM.